2007

Computational analysis of airfoils in ground effect for use as a design tool

Justin L. Smith
West Virginia University

Computational Analysis of Airfoils in Ground Effect For Use as a Design Tool

Justin L. Smith

Thesis Submitted to
The College of Engineering and Mineral Resources
at West Virginia University
in partial fulfillment of the requirements
for the degree of

Master of Science
in
Aerospace Engineering

James Smith, Ph.D., Chair
Wade Huebsch, Ph.D.
Greg Thompson, Ph.D.
Jacky Prucz, Ph.D.

Department of Mechanical and Aerospace Engineering

Morgantown, West Virginia
2007

Abstract

Computational Analysis of Airfoils in Ground Effect For Use as a Design Tool

Justin L. Smith

There has been interest shown in a recreational glider which operates primarily in the flight regime known as ground effect. Ground effect traditionally occurs when the airfoil is within a chords length of the ground. It is well known in the art that when the airfoil is present in ground effect the lift force is increased and the drag force is reduced on the lifting surfaces, in turn increasing the L/D ratio.

This recreational glider would have no internal power supply and only rely on the outside acting force. The considered force that would be used to propel this recreational glider would be the force of gravity pulling the craft down an incline. An incline such as this can be found at numerous ski resorts all over the world. The recreational glider could be used at these ski resorts year round and help solve revenue issues for ski resorts during the off season and provide a new recreational sport.

One of the major design aspects in designing the recreational glider is selecting an airfoil which will provide adequate lift in order to keep the craft airborne. At the same time this airfoil must allow for the most stable flight while maintaining the appropriate altitude in order to take advantage of the enhanced aerodynamic characteristics present in ground effect flight.

After the airfoil that would be used in the first design of the recreational glider was selected the airfoil performance was tested in Computational Fluid Dynamics (CFD). In order for this data to be trusted enough to invest the time and money into wind tunnel testing the CFD research needed validation. These results were then compared to the CFD results of previous experimental results.

Preliminary analysis indicated the Wortmann FX 63-137 provided a good first approximation and thus was analyzed for angles of attack of 0 to 6 degrees with height-to-chord ratios from 0.05 to 1, which determines the ground clearance of the airfoil. The airfoil was analyzed with the results obtained focused on the coefficient of lift, coefficient of drag, and the x-location of the center of pressure.

The CFD results showed that ground effect did increase the lift coefficient as the distance the airfoil above the ground was reduced. The results also showed that the drag coefficient was reduced as the distance the airfoil above the ground was reduced. These results were very evident at angles of attack of 4 and 6 degrees, and began to appear at an angle of attack of 2 degrees or less. The stability of the airfoil was also monitored by locating the center of pressure for the various angles of attack and altitudes. The center of pressure did not make any sudden shifts in location, instead making a slight move along the chord when the airfoil changed angles of attack.

This work leads to the following conclusions, and that was that the Wortmann FX 63-137 did show the increase in lift and reduction in drag when operating in ground effect that was expected, as well as minimal movement in the center of pressure along the chord length. This means that the airfoil can remain the initial airfoil to be used in the recreational glider, and proceed to experimental testing in order to verify the CFD results from this study.

Table of Contents

List of Figures

List of Tables

Nomenclature

AOA	Angle of Attack
C	Chord
C_d	Two dimensional coefficient of drag
C_l	Two dimensional coefficient of lift
CFD	Computational fluid dynamics
CIRA	Center for Industrial Research Applications
D	Drag
Fr	Froude number
H	Height
L	Lift
NACA	National Advisory Committee for Aeronautics
Re	Reynolds number

Symbols

g	Gravity
l	Length
L	Length
V	Velocity
ρ	Density
μ	Viscosity

Acknowledgements

The author would like to thank members of his committee, Dr. Greg Thompson, and Dr. Jacky Prucz, Dr. Wade Huebsch for his help in computational fluid dynamics questions and problems, and Dr. Jim Smith for directly supervising this project. The author would also like to thank Mr. Gerald Angle for assistance with various research issues as well as questions which would arise about the project.

The author would also like to thank his family for their support throughout his entire academic career, especially throughout college for all of their understanding and guidance along this long and difficult path.

Chapter 1.0 Introduction

Interest has been expressed in the development of a recreational glider that may be used in the flight regime known as the ground effect region. An airfoil is considered to be in ground effect flight when it is roughly within a chord's length distance from the ground. In this region, above the ground the lift that the wing produces is increased and a reduction in drag on the airfoil can be experienced as well. Aircraft which take advantage of these ground effect aerodynamics are not common in today's age of technology mostly due to the close proximity to the ground at which flight must occur.

The motivation for the design of this recreational glider was the way that birds fly in ground effect, most notably pelicans. Pelicans simply build up speed by using their wings, and then simply use the aerodynamic advantages present that close to the ground to glide over the water. They experience the same aerodynamic forces that an aircraft would face, which is enhanced lift combined with reduced drag during flight in ground effect.

The recreational glider under consideration would be designed with no propulsion system, thus outside forces must be applied to the vehicle in order for flight to occur. One way for this force to be created is by using gravity to essentially pull the glider down a slope. Slopes like the one being described are found at ski resorts all around the world and would be potential suitors for these recreational gliders.

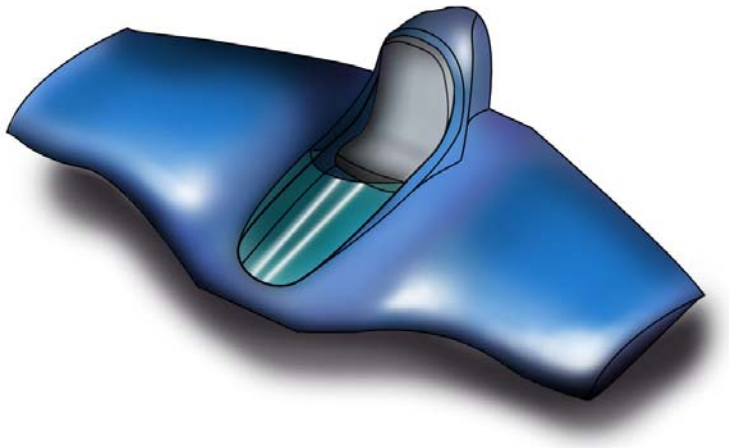

Figure 1: Artist Conception of Recreational Glider Currently Under Design by CIRA

Figure 1 above shows the initial conceptual design of the recreational glider being discussed. The craft shown is estimated to be approximately 10 ft long down the centerline, and have a tip chord of 6 ft., and the wing-span of this rough design is 12 ft. The weight of the glider is still under consideration due to design criteria, but the glider has been estimated not to weigh more than 60 lbs.

A major design concern in the design of this recreational glider is how to keep it in the air but at the same time make sure that it does not leave the ground effect regime. One of the ways to address this issue is to select an airfoil that will provide adequate aerodynamic performance characteristics, but at the same time maintain stable flight and will be sized to additional lift provided in ground effect to maintain flight.

Wind tunnel testing has long been a trusted method of experimental research for testing airfoil performance. The one downfall to wind tunnel research is that it can prove to be a costly operation as well as time consuming. Combining those two aspects and a research opportunity in a wind tunnel suddenly becomes a large part of a projects budget. With the advances being made in Computational Fluid Dynamics programs, otherwise

known as CFD, researches are beginning to trust data being output by these programs with accurate validation using this information to inexpensively and quickly advance design.

If these CFD research tools continue to progress forward in accuracy, researchers will be able to perform preliminary data in CFD in a more cost efficient manor before validating their preliminary results with experimental data. This approach of using CFD programs to analyze airfoils before experimentally testing a final design will be used in order to provide a starting point for designing the aforementioned recreational glider.

The purpose of this thesis is to recreate a ground effect experiment with a CFD model. The experimental results will then be compared to the CFD results to see how the coefficients compare to each other. The same techniques used to verify the selected experiment will then be used to analyze the airfoil which was previously selected to use in the first design of the recreational glider. The results of the selected airfoil CFD analysis will then be used to make decisions on how to advance the design further.

1.1 Research Objectives

The research objectives focus around two major ideas. This first objective is to select an experimental ground effect study which can be used to develop a CFD model which can be used as a design tool. The second objective is to use the techniques used in the experimental comparison CFD research in order to analyze the selected airfoil used by the recreational glider. The CFD study will focus on the coefficient of lift as well as the center of pressure location. The movement of the center of pressure is one of the early design concerns and needs to be modeled as accurately as possible.

Chapter 2.0 Literature Review

This chapter provides information on previous research performed in relation to this project. There have been both experimental and numerical studies on airfoils in ground effect throughout the years. Most of the studies performed used a stationary ground plane during experimentation; this issue however is beginning to be revisited when determining airfoil behavior when operating in ground effect conditions.

There are a few different reasons why this phenomenon occurs and why it is important for this study. As the velocity flow under the airfoil is decreased, pressure begins to build up on the lower portion of the surface. This higher pressure region under the airfoil will thus enhance the lift. The drag is also reduced due to a reduction in the induced drag on the airfoil. Both of these occurrences result in an overall increase in the L/D ratio of the airfoil [1].

2.1 Wing in Ground Effect Research

Wing in ground effect refers to an airfoil that is close enough to the ground so that it is being affected aerodynamically by the ground. The knowledge of the effects that the ground can have on airfoils dates back to the early 1920's. Early researchers were aware of the fact that the wing's resistance would be reduced when close to the ground and the lift would be slightly increased [2]. Researchers would begin by trying to simulate the ground inside of wind tunnels by using flat surfaces placed near the airfoil [3]. These methods were not the most accurate when trying to obtain results, but the researchers were still aware of this "cushion" of air that existed between the wing and the ground.

In the late 1920's full scale aircraft research began to look into ground effect in order to prove Wieselsberger's research correct. Vought VE-7 aircrafts were used in flight testing and were tested at altitudes far from the ground as well at altitudes as close to the ground as 5 feet. The results proved that the drag was reduced just as was assumed by Wieselsberger's theoretical work [4].

Research on ground effect was limited until designers began to think that they could take advantage of such a phenomenon. In the 1970's the United States and the Soviet Union both had an interest in flying wing vehicles. The United States had a desire to build a large transcontinental wing in ground effect vehicle. This aircraft would be able to carry more cargo than a Boeing 747, but not nearly as much as a ship. The idea of a hybrid airship providing improved performance when operating in ground effect seemed very economical [5].

This idea however was somewhat idled by the unveiling of Lockheed's C-5A transport [6]. In the early 1980's there were still efforts to try to push the idea of minimizing operating costs by use of a ground effect transport. Case studies suggested that since the new large transport aircraft couldn't increase much larger in size than they currently were, the only way to increase the size of the aircraft was to design them to fly in ground effect [7]. This idea never developed past early design phases and would be pushed to the side until the turn of the 21st century.

The Soviet Union also was a heavy player in the development of ground effect vehicles. The Soviets designed and built several vehicles that were designed to fly over water called ekranoplan. These programs however remained in very infantile stages and never continued production through the Cold War [6].

Presently there is research bringing back the notion of an intercontinental transport cargo aircraft that could operate in ground effect. Boeing Phantom Works is currently working on a cargo plane that would fly in ground effect as close as 20 feet above the ocean. An artist's conception of the Boeing Pelican can be seen below in Figure 2: Conceptual Design for Boeing Pelican [8]Figure 2. This plane would be able to carry up to 1,400 tons and would be about twice the size of the Russian An225 the world's largest aircraft [8].

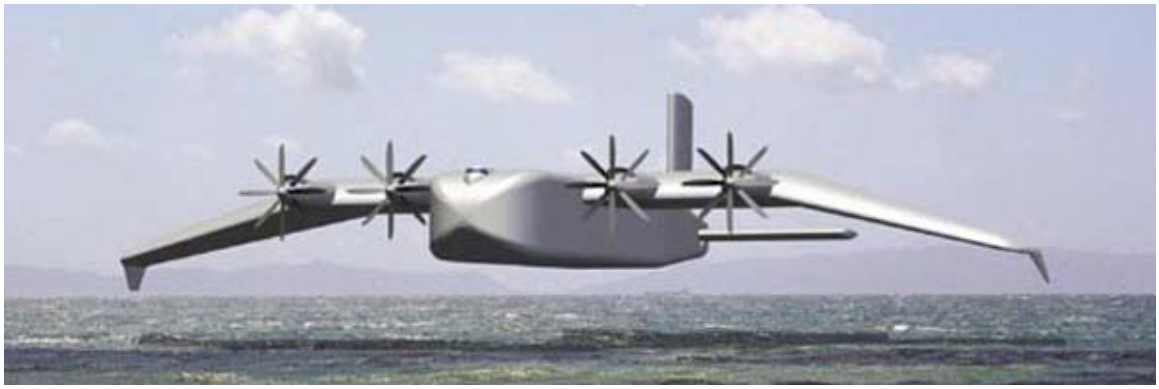

Figure 2: Conceptual Design for Boeing Pelican [8]

2.2 Experimental Research

Experimental research in ground effect has been subject to some controversy over the previous years. The research however has been proven to be questionable due to boundary effects. There have been experiments done with both a fixed ground plane, and a moving ground plane, which is the center of the debate and will be discussed further. The early research was performed primarily for specific cases, but recently there is experimental research being done for use as verification for CFD results.

In the mid 1970's research was performed by Ailor and Eberle on future ground transportation and the phenomenon of ram-lift under the body which is of interest. Several Geometry types were tested in both 3-D and 2-D experimentations and both sets

of tests showed that certain geometry shapes can generate significant lift when in ground effect [9].

In 1990 wind tunnel experimentation was performed on a wing with a NACA 4415 profile by Chawla, Edwards, and Franke. This research was performed in a wind tunnel which used boards to simulate the ground. The results from the study showed that the lift and drag coefficients were both increased when operating in ground effect [10]. This was in contrast to previous work done by Reid [4] where the drag was reduced as the altitude was decreased.

In 2002 Ahmed and Goonaratne performed research on an airfoil designed for a craft to fly in ground effect over water. This test was done with a fixed ground plane inside of a wind tunnel. The research proved that using flaps and end plates can prove to be beneficial while operating in ground effect [11].

Moving ground plane tests have been performed in order to perform ground effect research. Early 2-D experiments by Zerihan and Zhang were conducted to look at the downforce on inverted airfoils in ground effect. The results showed that the downforce was higher in the ground effect region around 20 percent chord than the values of the downforce at freestream [12]. Zerihan and Zhang moved on to study 3-D effects of turbulent wake and edge vortices a few years later. They concluded that the edge vortices help contribute to the increase in downforce while operating in ground effect. This shows that the rate of the change in downforce as the heights are adjusted can be directly linked to the vortex strength coming off the wing [13].

The most recent wind tunnel research which was performed was done in 2006 by Ahmed, Takasaki, and Kohama. Their research was focused on the aerodynamics of the

NACA 4412 airfoil in ground effect. This study was conducted by using a removable test section with a movable ground plane in a wind tunnel. The airfoil was tested at different altitudes within the ground effect flight regime in order to determine the changes in the aerodynamic performances. Their results show that for angles of attack greater than 4 degrees the lift was increased. Also they showed that the drag coefficient is higher the closer to the ground the airfoil is positioned [14]. This experiment shows the same results as the research done by Chawla, Edwards, and Franke; which shows the lift and drag increasing as the altitude decreases in a fixed ground plane experiment [10]. This research paper does however provide trends in the lift and drag coefficients similar to what would be experienced by a recreational glider.

2.3 Numerical Research

Numerical research has been the main focus of ground effect research since the early days of noticing the phenomenon. Most of the research being performed was done this way in order to study the aerodynamic behavior in ground effect without the use of or prior to experimental efforts. The questions being asked were how certain variances effect how the airfoil reacts in ground effect. At the same time these analytical studies were trying to prove discrepancies in experimental research that was being done in ground effect.

In 1965 Saunders explained irregularities in experimental and numerical research when considering ground effect. Through various models he showed that experimental results would not match numerical calculations if the boundary was stationary. Saunders reiterated accurate experimental techniques that may be used in order to verify numerical

solutions. The techniques that are considered to be better than a stationary ground plane according to Saunders are direct imaging with the airfoil and a towing method [15].

There were studies in fluid mechanics to research ground effect in the late 1970's. These studies were to show the effects of the flow at low Mach numbers and high Reynolds number. These studies focused on the extreme ground effect cases which can be experienced when a blunt body is at an approximate height-to-chord ratio as close to zero as possible [16]. This phenomenon of extreme ground effect does not behave like normal ground effect which is due to the fact that there is virtually no air under the lifting surface and should be considered when analyzing results in the study performed on the recreational glider wing.

In the mid 1980's numerical research was focused on predicting the location of the trailing vortex sheet [17]. Research was also performed numerically on the dynamic ground and changing height as an airfoil approaches the ground and how this effects the trailing edge vortices [18]. These vortices are directly linked to the influence of the ground on the flight of the aircraft. These equations were calculated with a thin wing and flat plate assumptions.

In 1989 there was numerical research focusing on the unsteady and steady ground effect with different wing planforms. Nuhait and Mook show that numerous aerodynamic parameters are affected by ground effect in both unsteady and steady flows. The coefficients were higher however in the unsteady flow than the steady flow [19]. In 1993 more numerical research was performed to further analyze the unsteady flow that is created when operating in ground effect. Their study used the vortex-lattice method using

flat plate approaching the ground [20]. This research was conducted as a focus on the aerodynamics during the take-off and landing portions of flight.

In 1996 numerical research by Coulliette and Plotkin used discrete vortex and vortex panel methods for research on how the angle of attack, camber, and thickness affect flight in ground effect. They too found the lift increasing as ground clearance diminishes, as well the fact that the lift is increased with the increasing thickness [21].

In 2003 there was numerical research on the vortex interaction with the ground during wing in ground effect flight. This model shows that vortices shed from an airfoil when operating in ground effect show interaction with the ground and thus affect the aerodynamics as well as pressure interaction with the ground [22].

Not only was the aerodynamics of ground effect flight being studied analytically but also the stability of aircraft in ground effect was a focus of some research. When the ideas of ground effect transport aircraft were in the early design stages, stability and control was an area of concern due to the differing flight characteristics of ground effect. Stability and control also was still a concern for commercial flight as well considering early on there was limited knowledge of this phenomenon [23]. This area has since expanded into even more modern day work with aircraft operating in ground effect.

In 2005 there was research done numerically to analyze the stability and performance of a winged vehicle which would fly in ground effect. Divitis used the Lagrange equations in order to analyze the forces and moments acting on the wing of the designed vehicle [24]. This research shows that stability and control research has been done on small aircraft which could fly in ground effect similar to a recreational glider.

2.4 Computational Research

In 1996 Hsiun and Chen set up computational research to be performed on the NACA 4412 Airfoil. This computational evaluation was performed in order to study the effect of Reynolds number as the airfoil operates in ground effect. The study was performed using the CFD PHEONICS code and also analytical equations. These studies were performed in a turbulent regime using the k-epsilon turbulence model [25].

This computational study compared the results obtained via computer to experimental results obtained earlier by Pinkerton. The study showed what was to be expected from an airfoil operating in ground effect during turbulent flow. The lift coefficient increased as the Reynolds number increased, and the drag coefficient decreased as the distance off the ground decreased [25].

Soon after this research, Steinbach critiqued the work of Hsiun and Chen by bringing up the fact that they used a stationary ground plane instead of a moving ground plane. The fact that the no slip boundary condition was used in the Navier Stokes Equations creates an error which can be avoided by using a slip condition. He suggests that they use the reflection of the airfoil in the flow so that the ground plane boundary layer will be avoided [26].

In 1999 Barber, Leonardi, and Archer stated that they too believe that in order to have accurate ground effect studies in CFD, the ground plane cannot be stationary. They described the four possibilities of reference frame to be: image (reflection of airfoil), slip (zero shear stress on ground), ground stationary, and ground moving with the same speed as the air. Of these four boundary conditions the most accurate one is the ground moving

at the same speed as the air due to the fact that this would be the closest boundary condition to what is really happening during wing interaction with ground effect [27].

In 2002 Barber, Leonardi, and Archer took previous ground effect research and reviewed the methods used during the research. They determined after CFD verification that if the research being performed was fixed body, then the only way to accurately predict ground effect behavior was to use the moving ground boundary condition. Other errors noticed by this study had to deal with flight over water, which in this case the non-uniform surface was another source of error [28].

In 2006 Barber conducted a case study of CFD and experimental experimentation. She goes on to discuss that her 2002 work showed that it was essential to use both numerical and experimental research in order to study ground effect. She goes on to reiterate that such experimental research is limited to specific situations which makes it difficult to establish faith in numerical simulations in other situations [29].

In 2003 Chun and Chang also questioned the accuracy of fixed ground plane simulations. The two researchers decided to perform CFD on both fixed and moving ground plane simulations in order to compare the accuracy of both to that of previous experimental work. They found through this comparison that the lift generated by both types of boundary conditions was similar each way. The drag however was different for each boundary condition; the drag was higher if the ground was moving. This drag difference can be linked to the boundary layer that would form on the fixed ground plane, which would affect the pressure distribution under the wing [30]

Chapter 3.0 Evaluation of Grid Setup

This chapter discusses the process of using an experimental procedure that has been performed in order to verify the techniques which will be used in a computational analysis. The first part of this chapter discusses the experiment that was chosen, and why it was chosen. The second part of this chapter discusses a computational comparison to the experimental setup. The third part of this chapter discusses the details of validating the CFD code using a grid independence check. The fourth part of this chapter discusses the results of the comparison to the experimental procedure by Ahmed, Takasaki, and Kohama [14].

3.1 Experiment Used for Grid Setup Evaluation

In order to validate the grid setup techniques that would be used in CFD it was necessary to use experimental research that has been done in the past and then recreate the experiment in CFD. The experiment that was chosen to be used as the validation case was an experiment by Ahmed, Takasaki, and Kohama [14].

In this experiment the gentlemen chose to analyze the aerodynamic characteristics of the NACA 4412 while in ground effect flight. This experiment was chosen because of the similarity to the computational research analyzing the selected airfoil being used by the recreational glider; the subject of this research.

The experiment used a moving belt system that could be moved in and out of a wind tunnel. This moving belt section simulates the fixed model moving through the air as mentioned in boundary condition papers discussed in section 2.4. The removable section consisting of the moving belt system, and the area where the test model was

placed was approximately 80 cm wide, 80 cm tall, and 100 cm long. Figure 3 shows the test section and the moving belt system which was used in the experimental setup for the NACA 4412.

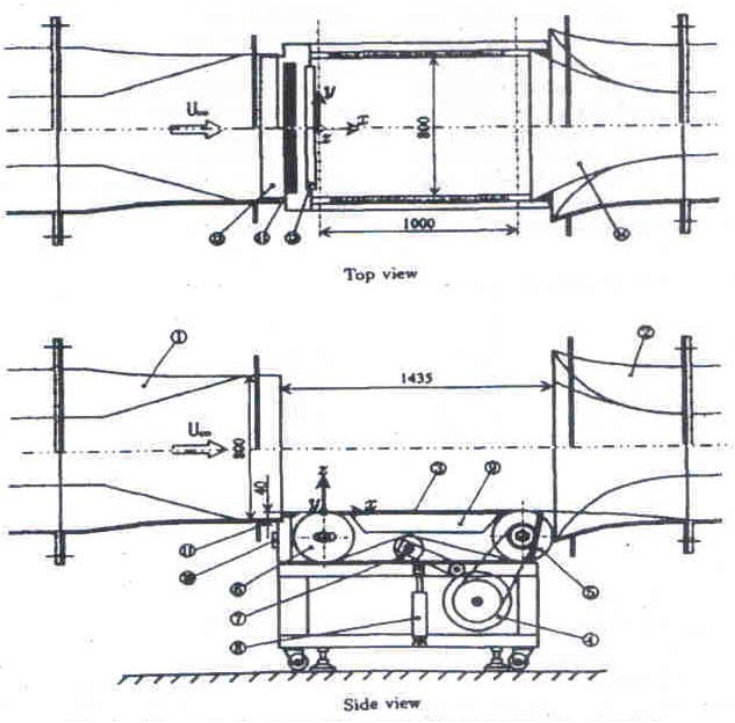

Figure 3: Test Section and Moving Belt System [14]

The test model that was used was a 60 cm span NACA 4412 airfoil with a chord length of 15 cm. The ends of this span were covered with end plates in order to simulate two-dimensional flow. The airfoil was tested at 6 different angles of attack; 0, 2, 4, 6, 8, and 10 degrees. Only the angles of attack of 0, 2, 4, and 6 were used in this comparison study as those where the angles of interest for the chosen airfoil. The setup of the airfoil inside of the test section can be seen below in Figure 4.

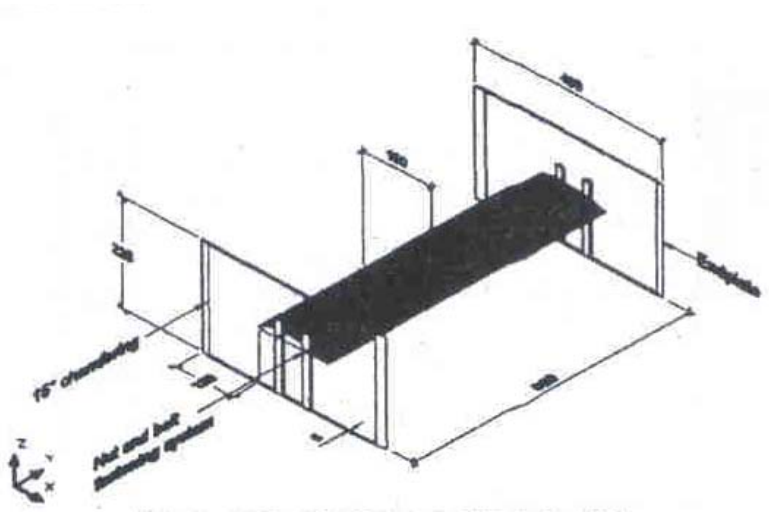

Figure 4: Test Model Setup [14]

At each angle of attack the airfoil was lowered to various heights from the surface of the belt to determine the strength of the ground effect at the different altitudes. The airfoil was fixed at a different distance from the belt each test, and this distance is in terms of height-to-chord length ratio. This distance was measured from the surface of the belt to the trailing edge of the airfoil. The ratios range from 0.05 to 1, which in this experimental case is from 0.75 cm to 15 cm. At the height-to-chord ratio of 1, the airfoil should be experiencing approximately the same conditions as free stream conditions.

The Reynolds number at which these tests were executed was 3×10^5, with an air and ground velocity of 30.8 m/s. This Reynolds number was selected due to its relevance to sailplanes, human powered vehicles, and unmanned air vehicles that all operate in ground effect [14]. This is the category of aircraft that the recreational glider being designed will fall into. The Reynolds number is very close to an approximate Reynolds number which has been previously calculated for the flight regime of the recreational glider.

3.2 Computational Setup

The experiment discussed in the previous section was setup in the geometry and mesh generation software Gambit 2.3.16. This tool provides a direct interface to the flow modeling software Fluent 6.2.16, which will be used to computationally analyze the flow. Two computers were used for computations; the first was a desktop computer with a 3.2 GHz Pentium 4 processor and 2 Gb of RAM. The second was a cluster of machines which was made up of 8 AMD Opteron 2.4 GHz dual core dual processor units, each containing 4 Gb of RAM, they were interconnected by gigabit Ethernet. The operating system which was being used on the desktop computer was Windows XP while the group of computers was operating on Windows server 2003. Each two dimensional flow analysis took approximately 2 hours for convergence criteria to be met in Fluent.

The geometry of the NACA 4412 airfoil was imported into Gambit, as well as the grid points which represent the dimensions of the test section. The grid structure was then created using an unstructured mesh. The grid sizing was determined after several different trials resulted in less accurate results. The specifics of the mesh are the same for every airfoil and every angle of attack. The number of grid points on each surface of the airfoil is 300, which is also consistent with each setup.

The grids that were created to be tested in Fluent were at 4 different angles of attack, 0, 2, 4, and 6 degrees. At each of those angles of attack there were also 7 different height-to-chord ratios, 0.05, 0.15, 3, 4, 6, 8, and 1. All of these different orientations of the airfoil are the same that were executed in the experiment that will be used for comparison. The primary reasoning behind this replication was to easily compare the computational results with the experimental results.

The following figure, Figure 5, shows the grid setup around the NACA 4412 airfoil when it is at an angle of attack of 2 degrees, and a height-to-chord ratio of 0.4. The other angles of attack grid setups can be found in the Appendix. The figure also can be used to describe the boundary conditions implemented into Gambit. In front of the airfoil the left boundary condition was set to a velocity inlet. Behind the airfoil the right boundary condition was set to be a pressure outlet. The ceiling above the airfoil was set to be a wall since it was far enough away from the airfoil to prevent any interaction. The lower boundary condition was also set to a wall, but in Fluent the wall can become a moving wall which was set to be the same speed as the velocity inlet.

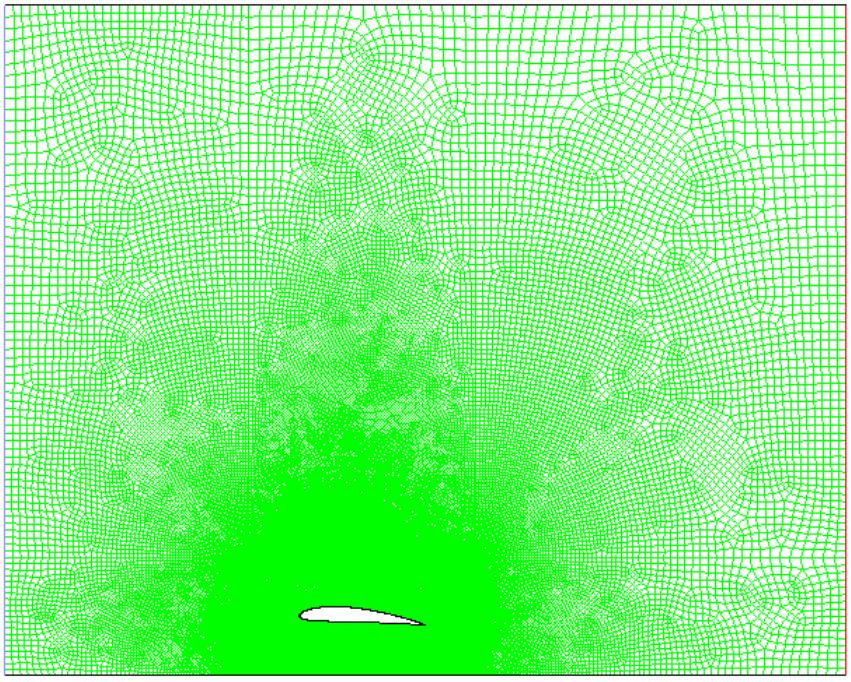

Figure 5: Grid Setup for NACA 4412 at AOA 2 deg H/C 0.4

Figure 6 shows a close-up of the grid surrounding the NACA 4412 airfoil when it is at an angle of attack of 2 degrees and a height-to-chord ratio of 0.4. Notice the collection of grid points focused on the front of the airfoil which is done to assure the flow is recreated as accurately as possible before the flow begins to separate from the

trailing edge of the airfoil. Figure 7 shows the cells around the leading edge of the airfoil in greater detail when locally enlarged.

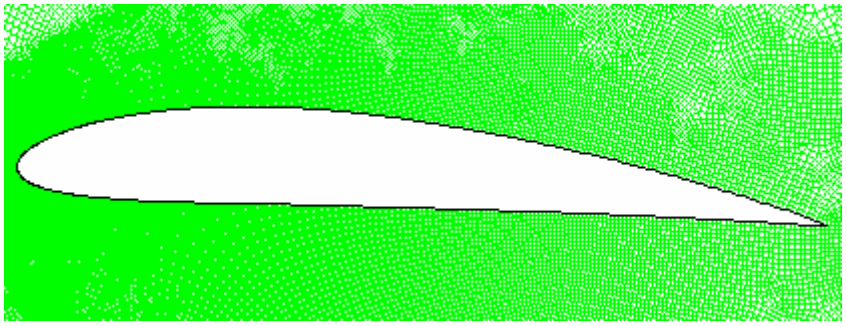

Figure 6: Close-up of Grid around NACA 4412 at AOA 2 deg H/C 0.4

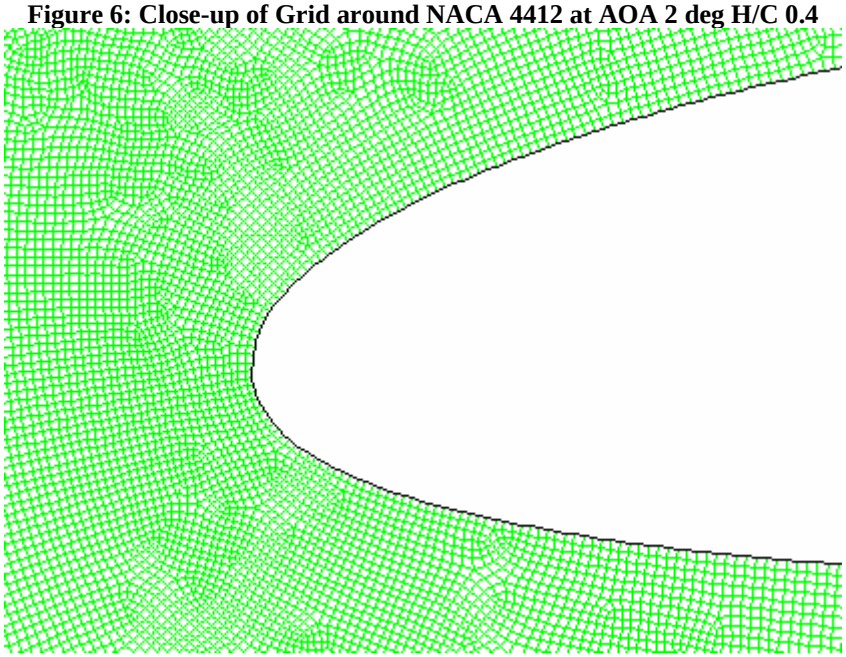

Figure 7: Leading Edge of NACA 4412 while at AOA 2 deg and H/C 0.4

After the various grids were implemented into Fluent, they could be analyzed by the flow modeling program. Each of these test cases would be treated as a laminar flow situation in Fluent. The following table, Table 1, shows the settings which were used in Fluent in order to analyze the flow.

Table 1: Fluent Settings for Experimental Comparison

Flow	Laminar
Solver	2-D Double Precision Segregated Solver
Momentum Equation Solver	First Order Upwind Discretization
Pressure Solver	PRESTO!
Energy Equation	Turned Off

The Reynolds number which was used in the experiment justified what the other constants to be implemented into Fluent. The velocity used in the experiment was 30.8 m/s, the Reynolds number was also known to be 300,000. From these numbers as well as the default values in Fluent for the density and the viscosity, the final constants could be determined.

The default value for the density was chosen to remain as it was at 1.225 kg/m^3, which meant that the viscosity must be changed slightly so that the Reynolds number remains $3x10^5$. After the Reynolds number equation, seen below in Equation 1, was rearranged to solve for the viscosity with the other values fixed, the value of the viscosity was determined to be $1.8865x10^{-5}$ kg/m-s which is the value of viscosity for standard air at 40^oC or 104^oF [31].

$$\mathrm{Re} = \frac{\rho V L}{\mu} \qquad (1)$$

The residuals: the continuity equation, u-velocity, and v-velocity, were all set to a convergence criterion of $1x10^{-9}$. The residual convergence was not the only means of convergence criteria, the lift and drag coefficients were also plotted and would create a flat line once the coefficient had converged. All of the trials converged at the aforementioned criteria in less than 4000 iterations; an example of this type of convergence can be seen in the Appendix.

The Reynolds number for this study indicates that the airflow is what is known as a transitional flow. It is known that this transitional flow is a transitional region between laminar and turbulent flow and normally occurs around a Reynolds number of $5x10^5$. These cases were all run in a laminar flow regime even though the Reynolds number indicated a transitional flow regime. The reason that only a laminar solver was used is

due to increase in drag over the airfoil caused by Fluent in a two dimensional analysis when applying a turbulent model to such a flow. Induced drag is higher during actual flight for a turbulent flow; Fluent however assumes that the entire flow is turbulent which is not the case for this low speed transitional flow.

In order to prove that the drag is increased significantly when a turbulent model is applied to the flow, several combinations of angles of attack and ground clearances were solved using the K-E turbulence model in Fluent. The results from these simulations proved that the use of a turbulent model introduces error which leads to inaccurate results. The results from each test showed approximately the same lift as the laminar solution, the drag however was much higher. The drag was so high due to an assumption being made by Fluent in the two dimensional analysis. The turbulence models add drag due to the assumption that the flow is fully attached to the airfoil, when in reality that is not the case.

The flow over the airfoil will separate from the airfoil as it enters the transition boundary layer; for low speed flows at a low angle of attack this happens near the trailing edge of the airfoil. When the turbulence model is applied in Fluent there is no way of pinpointing when or where the flow become separated, so the model assumes that the flow is attached the entire length of the airfoil and thus increases the drag dramatically.

The ideal case for such a transitional boundary layer would be to perform a laminar flow analysis over the majority of the aircraft, and then apply a turbulent flow model near the trailing edge of the airfoil. This would simulate what is occurring in the transitional boundary layer, as the laminar flow becomes turbulent flow over the airfoil.

Table 2 shows the values for the coefficient of drag for the 4 different angles of attack for the NACA 4412 airfoil at a height-to-chord ratio of 1. The percent difference in the drag coefficient produced by the turbulent model is remarkably higher than the results produced by the laminar model. These values show that the assumption of applying the turbulent model over the entire chord length of the airfoil is not appropriate for this transitional boundary layer case.

Table 2: Comparison of Turbulent and Laminar Models in Fluent

AOA	Experimental C_d	Laminar C_d	% Difference	Turbulent C_d	% Difference
0	0.00805	0.011496	42.81	0.053609	565.96
2	0.00912	0.012991	42.44	0.059670	554.28
4	0.01032	0.016190	56.88	0.076810	644.28
6	0.01200	0.022076	83.97	0.093287	677.39

This added drag was so high that it was decided that the solutions would actually be more accurate at velocities this low if the laminar solver was the only model applied to each case. These solutions were very close to the same results being shown in the experimental results which can be seen in the upcoming sections.

3.3 Validation of Fluent Results

Various grids were compiled in order to pick which grid would provide the most accurate flow analysis. The grid independence check was performed with several different grid points over the surface of the airfoil. The initial grid design consisted of 100 grid points on the surface of the airfoil. After the results were returned the number of grid points was increased to 200 grid points across the airfoil surface in order to see the repeatability of the results.

The next step was to up the number of grid points on the airfoil surface to 300 points in order to see if the solutions could be any closer to those being seen during the

experimental results. The results for 300 grid points were very close to the experimental results and therefore each trial would now use 300 grid points over the airfoil. Now a grid independence check needed to be done for 300 grid points. The number of grid points was increased to 350, 400, and 500 to see if repeatability could occur.

The lift coefficient was chosen to be the grid independence check for the different grid setups. Figure 8 shows the coefficient of lift as a function of the number of grid points for the airfoil at an angle of attack of 2 degrees for a height-to-chord ratio of 0.4. The figure shows the coefficient of lift converging after the number of grid points gets above 200.

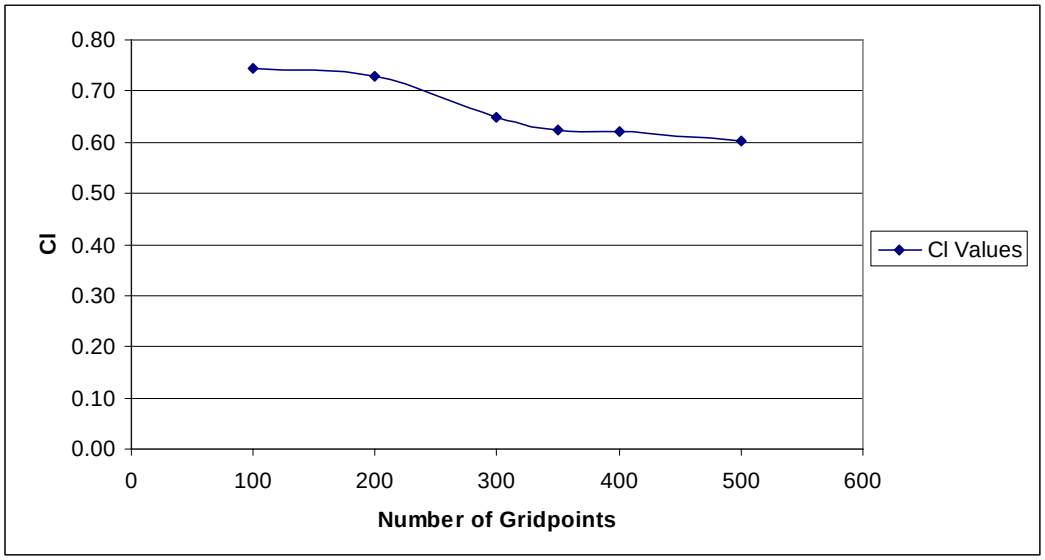

Figure 8: Coefficient of Lift vs Number of Grid Points for AOA 2 deg H/C 0.4

Table 3 shows the percent difference between the lift coefficients for the selected number of grid points of 300 and whatever the grid independence check number of grid points is. This angle of attack and height-to-chord ratio setup was chosen due to the fact that the values for the lift coefficients were the closest to those achieved in the experimental results for low angle of attack.

Table 3: Grid Point Comparison of NACA 4412 for AOA 2 deg H/C 0.4

# of Grid Points	% Difference in C_l
100 and 300	14.50
200 and 300	12.28
350 and 300	4.17
400 and 300	4.70
500 and 300	7.46

Table 3 shows that the percent difference is reduced every time the number of grid points are reduced. The percent difference from 300 to 350 grid points was slightly under 5 % and the difference between 350 and 400 grid points was less than 1 %. The overall percent difference from the chosen 300 grid points to the highest number of grid points was only 7.46 %.

3.4 Results of Experimental Comparison

The results from the Fluent trials were compiled and put into table format comparing the coefficients of lift and drag. The tables list the height-to-chord ratios, the lift and drag coefficients, and the percent difference between the C_l and C_d values from the experiment and the CFD computations. The first comparison between the experimental results and the CFD results from Fluent is shown in Table 4.

This comparison is for the NACA 4412 airfoil at an angle of attack of 0 degrees. The percent difference between the experimental and CFD results with the largest percent difference occurs at the C_l value for a height-to-chord ratio of 0.05, which is 7.5 mm off of the moving belt's surface. This minimal distance at which the trailing edge is above the surface puts the front part of the airfoil even closer to the ground. The fact that the front of the airfoil is so close to the ground allows the majority of the air to go across the top of the airfoil and virtually no air passes between the lower surface of the airfoil and

the belt. This phenomenon was noticed in extreme ground research done by Tuck where the height-to-chord ratio was as close to zero as possible [16]. The averages for the lift and drag coefficients were calculated without using the values for the height-to-chord ratio of 0.05. The average percent difference for the C_l values excluding the first case was 4.76%, and the average percent difference for the C_d values excluding the first case was 37.07%.

Table 4: Comparison of Experimental and CFD Results for AOA 0 degrees

C_d		H/C	C_l			% Difference	
Exp.	CFD		Exp.	CFD		Cd	Cl
0.00848	0.014409	**0.05**	0.024	-0.050		69.91	306.39
0.00826	0.010937	**0.15**	0.371	0.359		32.40	3.19
0.00815	0.010793	**0.3**	0.418	0.415		32.43	0.74
0.00805	0.010893	**0.4**	0.442	0.423		35.32	4.33
0.00805	0.011125	**0.6**	0.450	0.427		38.19	5.02
0.00805	0.011371	**0.8**	0.458	0.427		41.26	6.82
0.00805	0.011496	**1**	0.474	0.434		42.81	8.43
					avg	37.07	4.76

The following figure, Figure 9, shows the C_l values over the varying ground clearances for the experimental trials and the CFD trials. The figure shows the points at the height-to-chord ratio of 0.05 which show the extreme ground effect trends described by Tuck [16]. The C_l value from the experimental results also show extremely low lift values. The experimental data shows an increase of lift as the height-to-chord ratio approaches 1. The CFD results show a relatively constant value of lift after the height-to-chord ratio of 0.3.

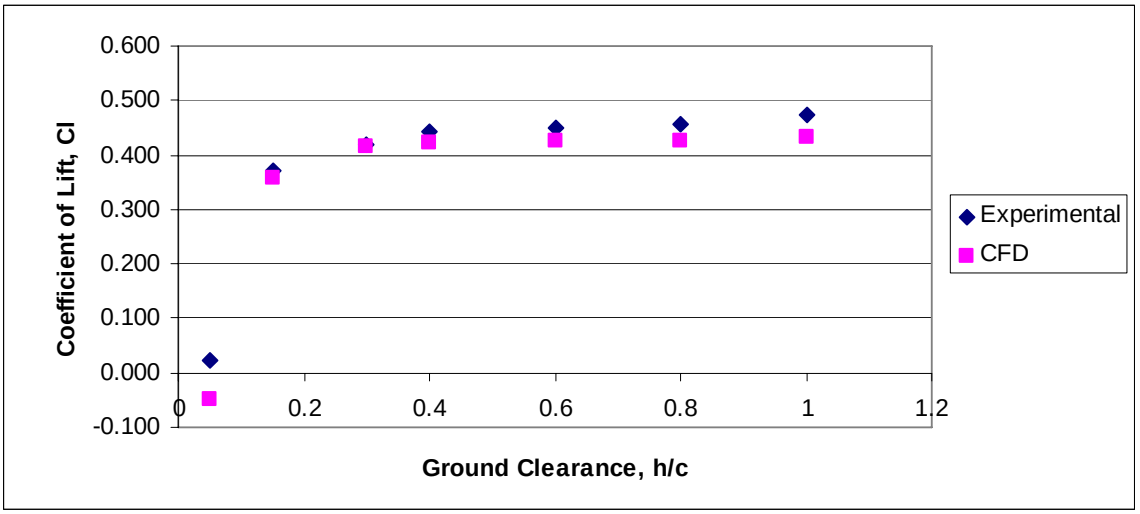

Figure 9: Coefficient of Lift of NACA 4412 at AOA 0 deg

Figure 10 shows the C_d values over the varying ground clearances for the experimental trials and the CFD trials. The experimental values show a slight decrease in drag as the height-to-chord ratio increases. The CFD results show a slight increase in drag as the height-to-chord ratio increases due to reduction in induced drag.

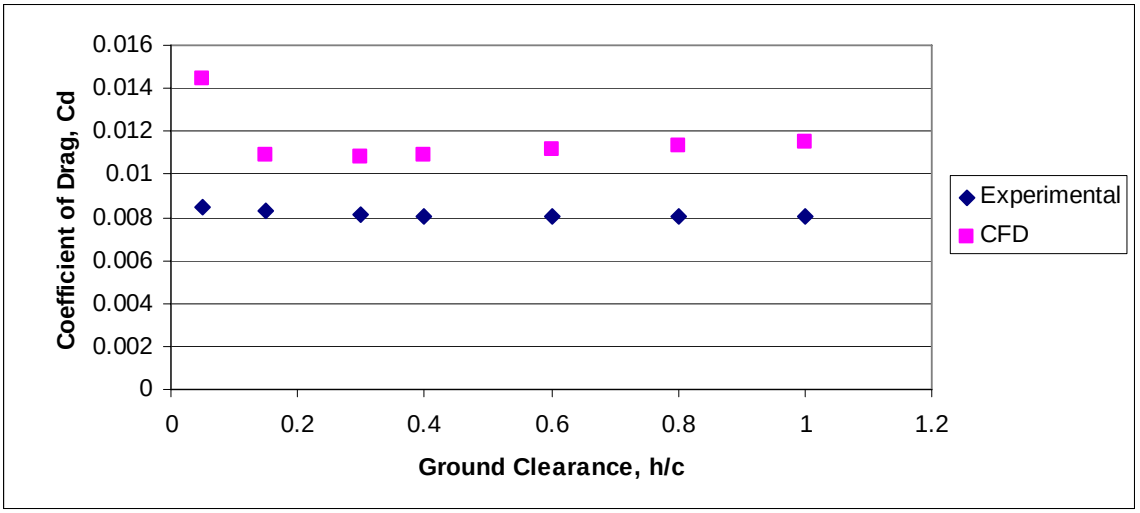

Figure 10: Coefficient of Drag of NACA 4412 at AOA 0 deg

Table 5 provides a numerical comparison between the values for C_l ad C_d for the experimental and CFD results at an angle of attack of 2 degrees. Again the largest area of concern for a percent difference is the C_l value at a height-to-chord ratio of 0.05. The fact that the airfoil is at an angle of attack of 2 degrees provides some air to flow underneath

the airfoil, but at the same time this small gap could be restricting air flow which would result in the high percent difference experienced at this height-to-chord ratio. This trial overall was very close to matching the results of the experiment as can be seen in the percent differences. The average value for Cl even with the first height-to-chord ratio error is still 7.26%, and the average value of C_d value is 30.68%.

Table 5: Comparison of Experimental and CFD Results for AOA 2 degrees

C_d		H/C	C_l			% Difference	
Exp.	CFD		Exp.	CFD		Cd	Cl
0.00957	0.011326	**0.05**	0.624	0.748		18.35	19.94
0.00935	0.011440	**0.15**	0.632	0.681		22.35	7.81
0.00935	0.011814	**0.3**	0.647	0.649		26.35	0.31
0.00924	0.011877	**0.4**	0.655	0.651		28.54	0.67
0.00912	0.012303	**0.6**	0.663	0.632		34.90	4.68
0.00912	0.012938	**0.8**	0.679	0.626		41.86	7.87
0.00912	0.012991	**1**	0.686	0.621		42.44	9.51
					avg	30.68	7.26

The lift coefficients obtained at the angle of attack of 2 degrees were plotted in Figure 11. From the Experimental results again there is an increase in lift as the height-to-chord ratio approaches 1. The CFD results begin to show the characteristics of ground effect flight as the values of C_l slightly decrease as the height-to-chord ratio approaches 1.

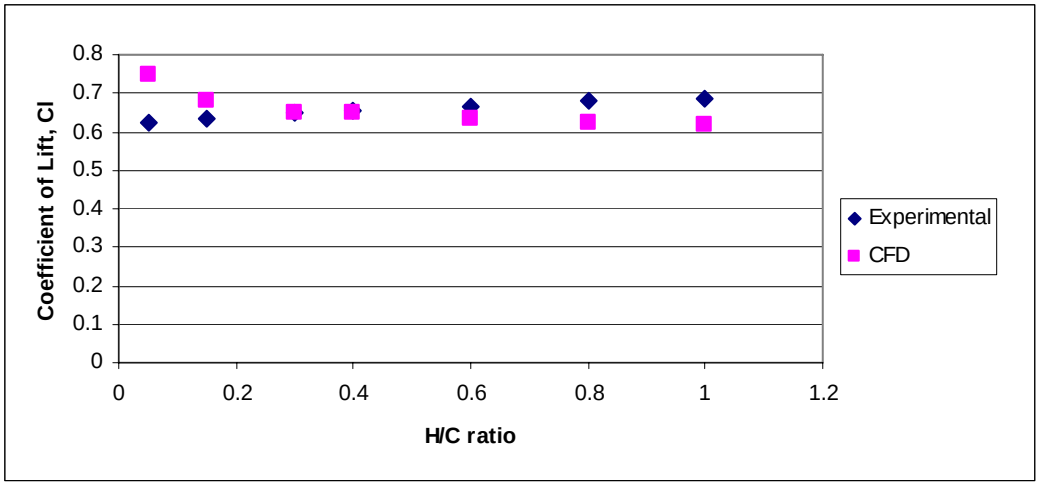

Figure 11: Coefficient of Lift of NACA 4412 at AOA 2 deg

The trends of the values of C_d plotted in Figure 12 show the characteristics of ground effect flight in the CFD results, which is the drag decreasing as the airfoil approaches the ground, after the airfoil is 12 cm above the ground the coefficient of drag becomes constant. The experimental C_d values are relatively constant and show a very slight decrease in value when the airfoil is above 6 cm off the belt's surface; the drag coefficient at 6 cm off the belt is 0.00924, and at 15 cm off the belt's surface is 0.00912.

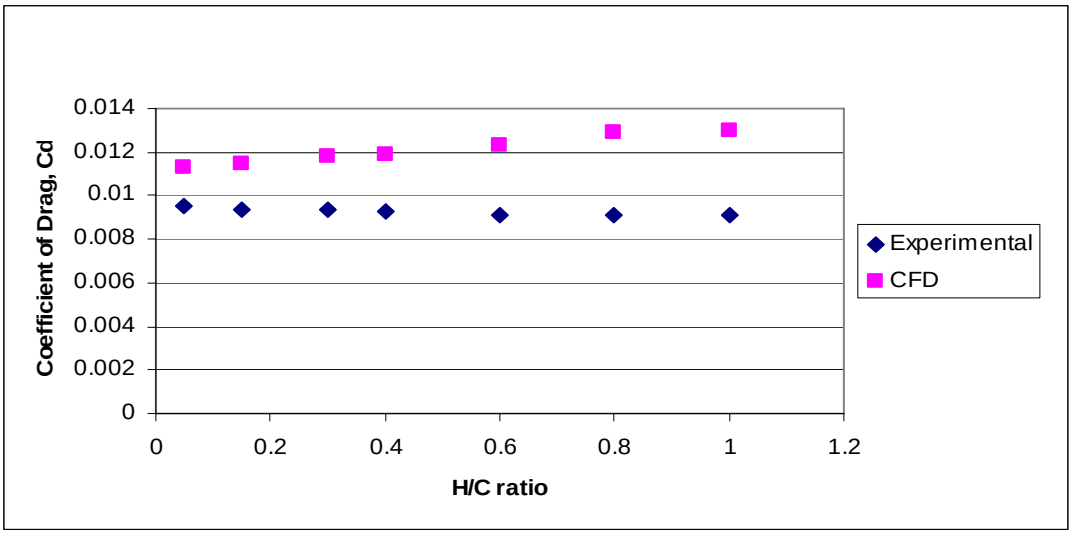

Figure 12: Coefficient of Drag of NACA 4412 at AOA 2 deg

Table 6 shows the comparison of the experimental and CFD results at an angle of attack of 4 degrees. The largest C_l percent difference again is at the height-to-chord ratio of 0.05. The other C_l values from the CFD results are very close to the C_l values found in the experimental data. The average percent difference for the Cl values is 9.04 % which includes the high percent difference achieved at the height-to-chord ratio of 0.05. The average percent difference for the C_d values is 43.17%.

Table 6: Comparison of Experimental and CFD Results for AOA 4 degrees

C_d		H/C	C_l			% Difference	
Exp.	CFD		Exp.	CFD		Cd	Cl
0.01130	0.014980	**0.05**	0.865	1.092		32.52	26.29
0.01109	0.014881	**0.15**	0.868	0.919		34.22	5.87
0.01087	0.014953	**0.3**	0.881	0.856		37.57	2.83
0.01076	0.015468	**0.4**	0.884	0.846		43.74	4.24
0.01065	0.015606	**0.6**	0.897	0.822		46.51	8.29
0.01043	0.015733	**0.8**	0.900	0.819		50.78	9.05
0.01032	0.016190	**1**	0.875	0.816		56.88	6.72
					avg	43.17	9.04

Figure 13 analyzes the airfoil at an angle of 4 degrees, which is when ground effects should be present and distinguishable. The experimental results show a decrease in lift as the airfoil gets closer to the ground, where as the CFD results show that the lift is slightly increased closer to the ground. The lift coefficient becomes constant after the height-to-chord ratio of 0.4.

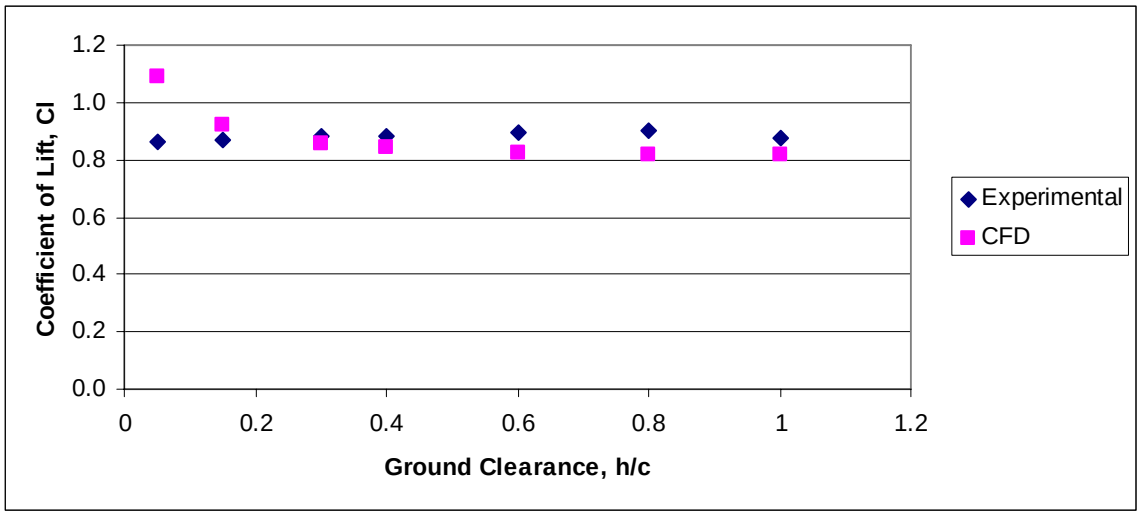

Figure 13: Coefficient of Lift of NACA 4412 at AOA 4 deg

Again the presence of ground effect should be evident at an angle of attack of 4 degrees which should mean a slight reduction in drag the closer the airfoil gets to the ground. The experimental results which can be seen in Figure 14 do not reflect this trend, as they show a very slight increase in drag as the airfoil gets closer to the ground. The

CFD results show that the drag is slightly decreased as the airfoil approaches the ground which was shown in earlier work.

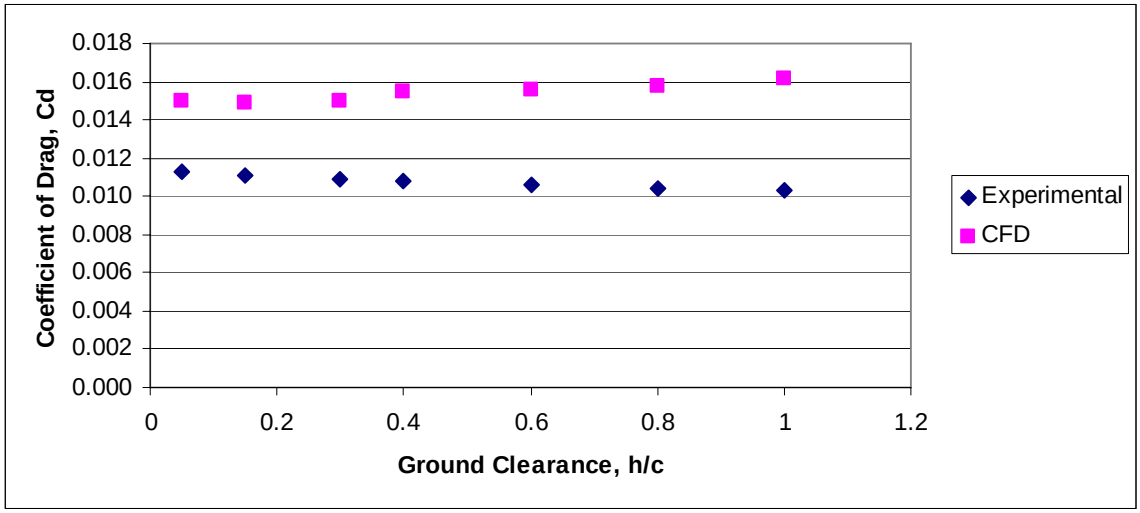

Figure 14: Coefficient of Drag of NACA 4412 at AOA 4 deg

The last angle of attack that was studied was 6 degrees, the results from these trials can be found in Table 7. The largest percent differences for the C_l values during this trial occurred during the final few height-to-chord ratios. One reason for this is possibly traced to the experimental results. The values obtained for the C_l values for all of the height-to-chord ratios experienced little change, this phenomenon can be seen in Figure 15. Another potential reason for this difference is the laminar flow model used in Fluent. The flow at 6 degrees angle of attack should be transitioning into more of a turbulent flow. If the turbulent model is used then introduction of other problems becomes an issue as was discussed earlier. The percent difference average for the value of C_l at this angle of attack is 9.88 %, and the percent difference average for the value of C_d is 62.06 %.

Table 7: Comparison of Experimental and CFD Results for AOA 6 degrees

C_d		H/C	C_l			% Difference	
Exp.	CFD		Exp.	CFD		Cd	Cl
0.01446	0.022490	**0.05**	1.090	1.203		55.57	10.41
0.01391	0.021177	**0.15**	1.090	1.044		52.21	4.13
0.01348	0.020240	**0.3**	1.090	0.994		50.17	8.79
0.01304	0.020283	**0.4**	1.082	0.979		55.50	9.52
0.01261	0.020235	**0.6**	1.082	0.974		60.48	9.93
0.01196	0.021109	**0.8**	1.082	0.963		76.55	11.00
0.01200	0.022076	**1**	1.096	0.927		83.97	15.38
					avg	62.06	9.88

Figure 15 shows the very interesting results from the angle of attack of 6 degrees. The experimental results clearly show a constant lift coefficient, which for an angle of attack does not seem to be accurate. The CFD results trend line show higher C_l values the closer the airfoil is to the ground.

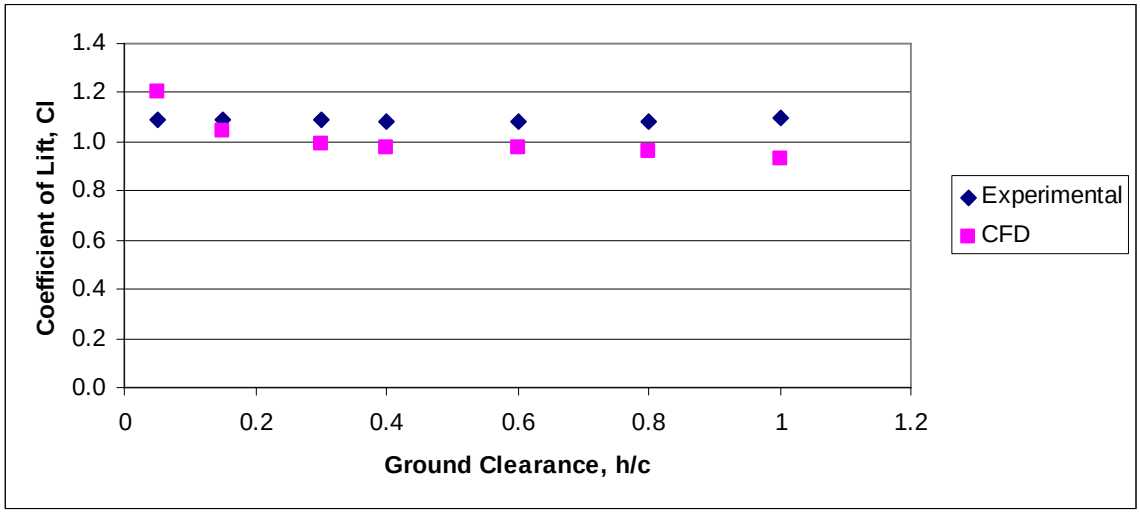

Figure 15: Coefficient of Lift of NACA 4412 at AOA 6 deg

The values of C_d which were plotted in Figure 16 show the same trend for when the airfoil is within 6 cm of the ground, and that is a increase in drag the closer the airfoil is to the surface. When the airfoil is above 6 cm from the ground the experimental results show that the drag continues to reduce as the height-to-chord ratio approaches 1. The CFD results show an increase in drag as the height-to-chord ratio is increased.

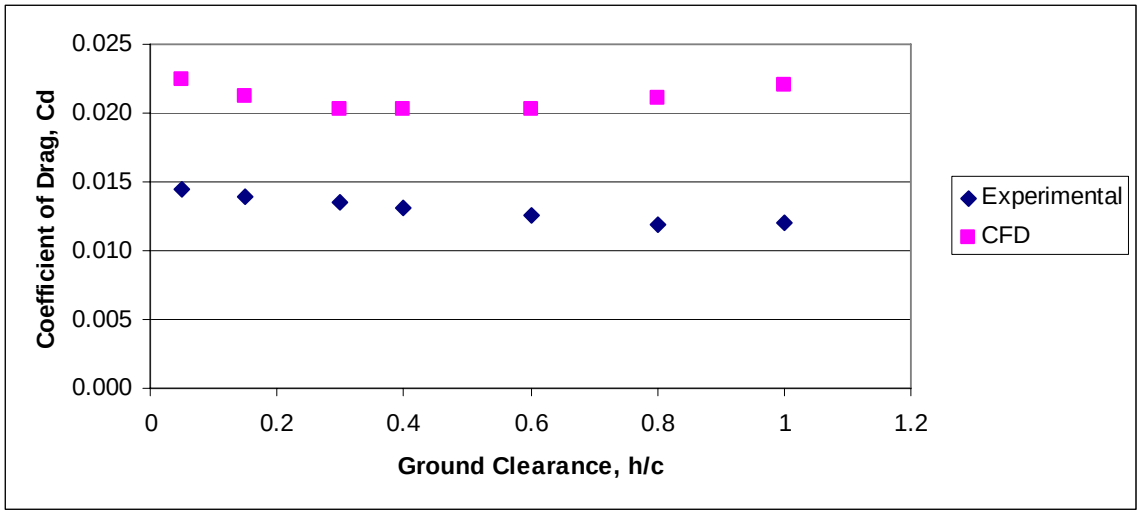

Figure 16: Coefficient of Drag of NACA 4412 at AOA 6 deg

The values for all of the above tables can be compared to free stream flight conditions by using the values obtained from the Theory of Wing Sections [32]. These values were taken at a slightly higher Reynolds number, but the values for the coefficients at the height-to-chord ratio of 1 should be approaching free stream air conditions.

Table 8 shows the percent differences between both the experimental and computational results for the airfoil at the height-to-chord ratio of 1. The lift coefficients are all under 10 % difference of the free stream conditions for the CFD results. The lift coefficients for the experimental results are all under 20 % difference.

Table 8: Lift Coefficient Comparison of H/C of 1 and Free Stream Conditions

AOA	Exp.	Book	% Difference	CFD	Book	% Difference
0 deg	0.474	0.4	18.5	0.434	0.4	8.5
2 deg	0.686	0.6	14.3	0.621	0.6	3.5
4 deg	0.875	0.84	4.2	0.816	0.84	2.8
6 deg	1.096	1.02	7.5	0.927	1.02	9.1

Table 9 shows the drag coefficient comparison between both the experimental and computational results and the free stream air conditions given by Abbott and Von Doenhoff [32]. The percent differences for the drag comparison were much higher for

both the experimental and computational results. This could be from the fact that the free stream results were taken at a higher Reynolds number of $3x10^6$ as apposed to the Reynolds number that was used in the study.

Table 9: Drag Coefficient Comparison of H/C of 1 and Free Stream Conditions

AOA	Exp.	Book	% Difference	CFD	Book	% Difference
0 deg	0.0081	0.0068	19.3	0.0115	0.0068	70.3
2 deg	0.0091	0.0069	32.2	0.0130	0.0069	88.3
4 deg	0.0103	0.0070	47.4	0.0162	0.0070	131.3
6 deg	0.0120	0.0083	44.6	0.0221	0.0083	166.0

All of the lift coefficient values for the experimental results were plotted in Figure 17. Again as discussed earlier experimental values showed that the lift slightly decreased for the airfoil the closer it was to the ground. For the angle of attacks of 4 degrees and 6 degrees, the values for C_l were essentially constant. This result should not be present due to the higher angle of attack and the presence of ground effect.

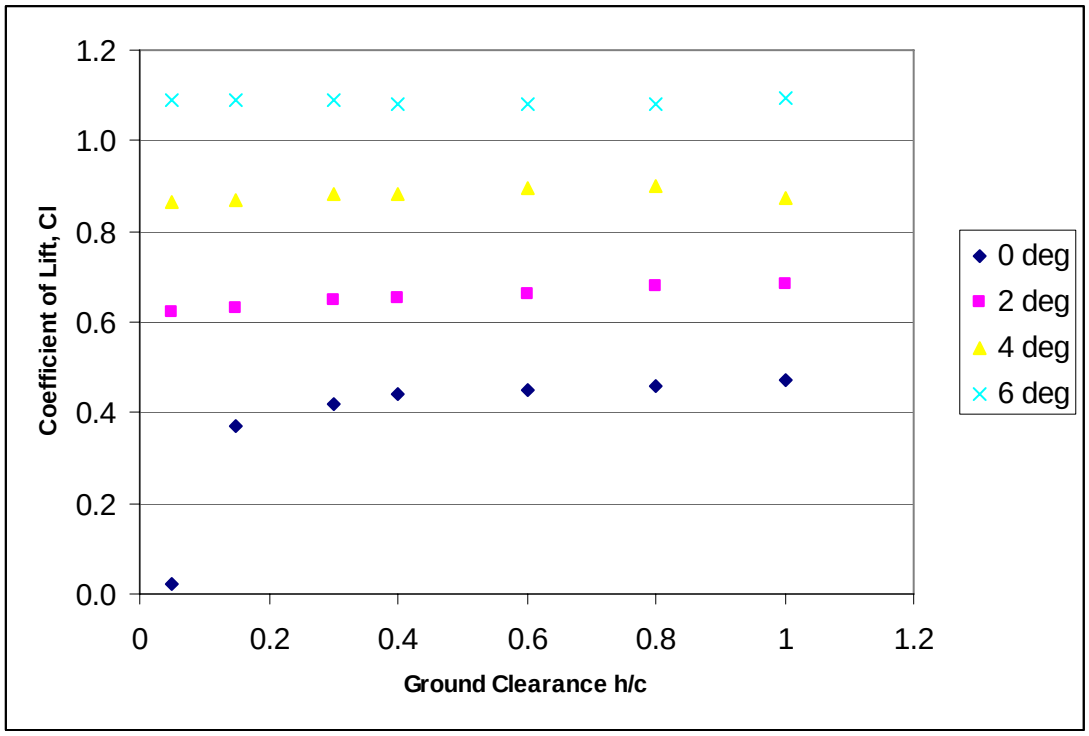

Figure 17: Coefficient of Lift of NACA 4412 for Experimental Results

All of the values for the drag coefficient for the experimental results were plotted in Figure 18 for the 4 different angles of attack in order to show the general trends being shown by the NACA 4412 airfoil during the experimental results. As previously stated for the experimental results the drag is increased as the angle of attack is increased. The drag is even further increased as the airfoil is lowered closer to the ground.

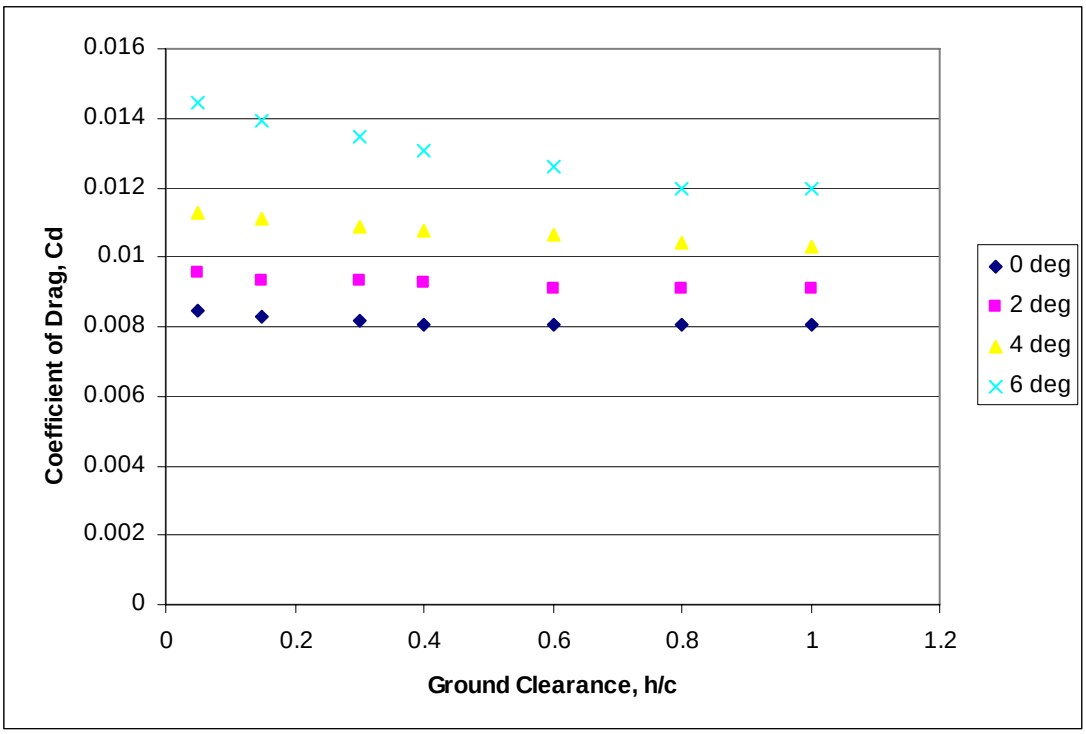

Figure 18: Coefficient of Drag of NACA 4412 for Experimental Results

The lift and the drag coefficients do not show the normal behavior of airfoils operation in ground effect. This however does not mean that the value is wrong or not useful. There were possible sources of error introduced during the experimentation as well as during interpretation. The experiment used end plates over the end of the 60 cm wing segment in order to simulate 2-D flow; this could have possibly introduced error into the flow around the airfoil particularly in ground effect.

The values of the lift and drag coefficients were also interpolated by hand using a ruler and scaling the values with the given axis. This is another source of introduced error other than the possible errors that already could have exited due to experimentation setup and evaluation.

Another possible explanation of discrepancies is how the geometric model was set-up in Gambit. The model which was analyzed was a two dimensional view of the test setup, when in reality it was a three dimensional test which used endplates to simulate a two dimensional result. If the model was created as a three dimensional geometry and treated as a three dimensional flow in Fluent then the flow would behave more like the flow behaved in the experiment.

In order to see if a three dimensional flow analysis in CFD would agree more with the experimental results, one three dimensional case was ran. The chosen case was the NACA 4412 airfoil at an angle of attack of 0 degrees and a height to chord ratio of 0.4. The results of this three dimensional analysis can be seen in Table 10. These results show that the drag coefficient difference was reduced to less than 3%. This trial shows that in order to truly recreate the experiment, the geometry should be constructed in three dimensions. This project was not able to analyze every test as a three dimensional flow due to computational time. A three dimensional analysis took approximately 3 to 4 days in order to mesh the geometry in Gambit and run the analysis in Fluent. This would have taken approximately 3 to 4 additional months of work per airfoil.

Table 10: 3-D Analysis of NACA 4412 Comparison

	C_d		H/C	C_l			% Difference	
Trial	**AIAA**	**CFD**		**AIAA**	**CFD**		**Cd**	**Cl**
3-D	0.00805	0.007859	**0.4**	0.442	0.4548		2.37	2.90
2-D	0.00805	0.010893	**0.4**	0.442	0.423		35.32	4.33

This study did not have control over the experimental results but assumes the trends to be an accurate indication of the actual airflow properties. This study hoped to show the same types of trend for CFD analysis and thus provide a tool for future design efforts for the recreational glider being considered. The trends which were produced in the two dimensional analysis should provide a good reference in order to select a geometric setup which could be further analyzed in a three dimensional setup.

Chapter 4.0 Computational Analysis of Selected Airfoil

This chapter discusses the computational analysis of the selected airfoil for the recreational glider. The first part of this chapter discusses the grid setup of the airfoil. The second part of the chapter discusses the methods used to analyze the airfoil computationally.

4.1 Grid Setup of Selected Airfoil

The airfoil which was selected to be used in the initial design of the recreational glider was the Wortmann FX 63-137. This airfoil was modeled in the grid generation tool Gambit 2.3.16, in order to then be analyzed using Fluent 6.2.16. The methods used to model this airfoil were the same as the methods used to model the NACA 4412 airfoil from the previously discussed experiment.

The geometry of the Wortmann FX 63-137 was imported into gambit. The airfoil's chord length was set to 1 meter for the computational analysis; this was done in order to simplify analytical calculations when relating the velocity used by the full size recreational glider to the velocity which should be used in the computational setup. The geometry of the test section around the airfoil was scaled up from the dimensions of the test section used in the experiment. The reason the test section was scaled up is due to the chord length used in the experiment being only 15 cm.

The grid sizing that used for the airfoil was the same that are used for the experimental comparison. There were 300 grid points across each surface of the airfoil, which was used for each angle of attack at each height. The heights that this airfoil was tested at were the same ratios as used in the experiment. Those height-to-chord ratios

were: 0.05, 0.15, 0.3, 0.4, 0.6, 0.8, and 1 which again represent the distance measured from the surface to the trailing edge of the airfoil. In this computational study with a chord length of 1 meter the distance from the surface to the airfoil were: 5, 15, 30, 40, 60, 80, and 100 cm.

The selected airfoil was analyzed at several different angles of attack in order to establish a fixed angle position which could be used for the initial design. The angles of attack which will be used for testing are 0, 2, 4, and 6 degrees. At each tested angle of attack different distances from the ground were also tested to see where the most optimum altitude for flight would occur. Under standard assumption of ground effect this altitude would be somewhere below a height-to-chord ratio of 1.

The following figures show the airfoil at the same orientation and grid setup which was used for the NACA 4412 in the experimental comparison. Figure 19 shows the grid setup as well as the boundary conditions of the mesh which are the same as the experimental comparison. The other grid setups for the different angles of attack can be found in the Appendix. The left boundary condition was a velocity inlet which was set to 7.8686 m/s. The right boundary condition was a pressure outlet, and the ceiling was set to a wall boundary condition. The lower boundary condition, which was the ground, was also set to a wall boundary condition. This wall was also set to be a moving wall; the speed of this wall was set to be equal to the velocity inlet at 7.8686 m/s. This reasoning behind this velocity will be explained further later in this chapter.

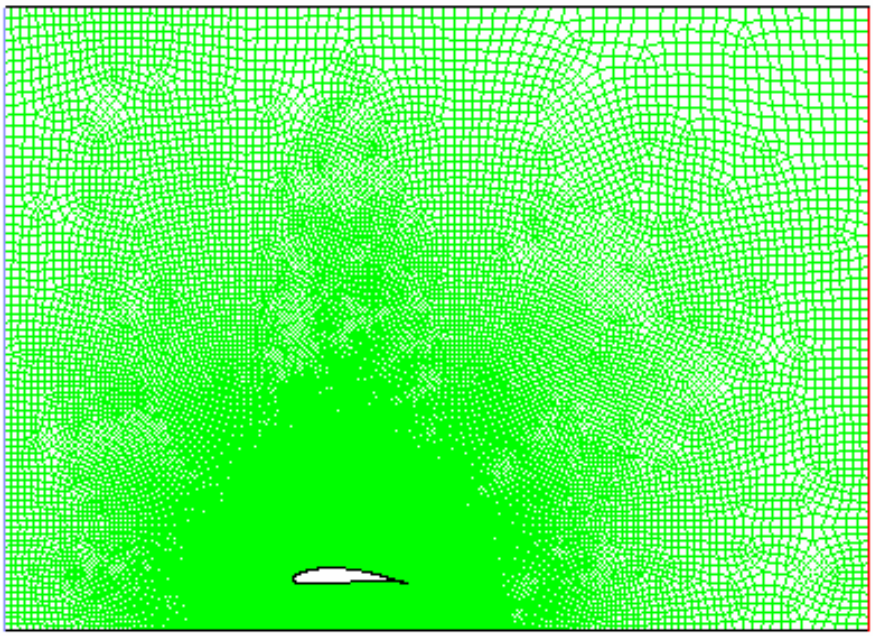

Figure 19: Grid Setup for Wortmann FX 63-137 at AOA 2 deg H/C 0.4

Figure 20 shows the grid points located around the airfoil, as well as a better view of what the Wortmann FX 63-137 Airfoil looks like. Notice the very sharp trailing edge as compared to the NACA 4412 airfoil from the experimental procedure. The airfoil is also at an angle of attack of 2 degrees, which shows that the airfoil has more of a rounded bottom as compared to the NACA airfoil. This concavity under the airfoil allows for more pressure build up and thus results in the airfoils higher lift coefficients. Figure 21 shows a focused view of the airfoil, and allows for the viewing of the individual cells surrounding the leading edge of the airfoil.

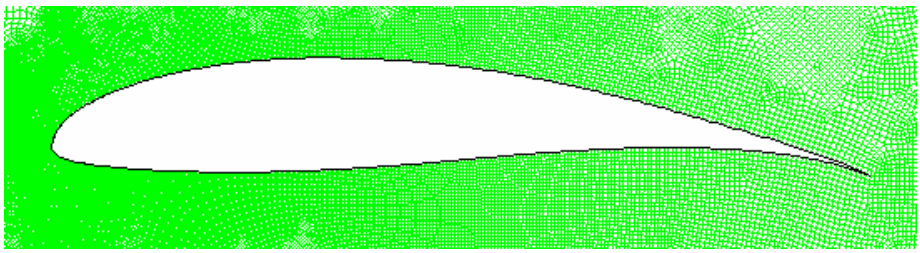

Figure 20: Close-up of Grid around Wortmann FX 63-137 at AOA 2 deg H/C 0.4

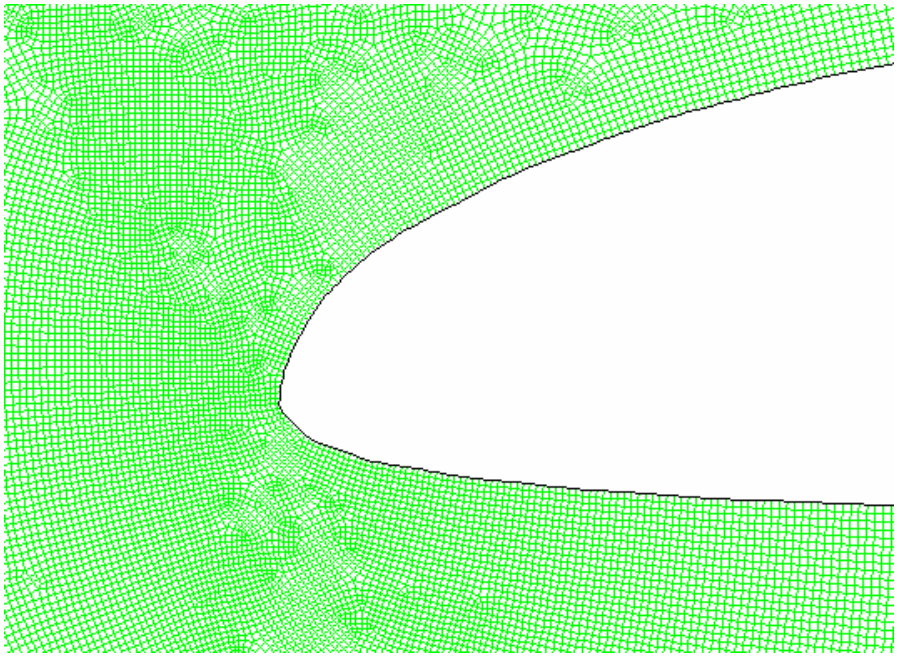

Figure 21: Leading Edge of Wortmann FX 63-137 while at AOA 2 deg and H/C 0.4

After the geometries were implemented into Gambit, and the mesh files exported into Fluent, the same settings were used in Fluent that were used for the experimental comparison. These settings can be found in Table 1. The values of density and viscosity remained set to the default values of 1.225 kg/m^3 and 1.7682 kg/m-s respectfully. The velocity value which was to be used was an educated guess as to what velocity range that the recreational glider would be operating in order to stay in the air.

The initial guess as to what the average chord length of the recreational glider would be was an 8 ft chord. This length and an estimated velocity of 40 ft/s was used to relate what the velocity needed to be over a scaled down chord length of 1 meter. The equation used to relate the velocities and chord lengths was the Froude number equation seen below in Equation 2.

$$Fr = \frac{V}{\sqrt{gl}} \qquad (2)$$

This relation was used because the Froude number is a dimensionless group used for flow with a free surface. The velocity of 40 ft/s for the 8 ft chord was scaled down to 7.8686 m/s by setting the Froude Numbers equal to each other.

Chapter 5.0 Results of Wortmann FX 63-137 Study

The computational study which was conducted on the Wortmann FX 63-137 focused on looking at lift and drag coefficients as well as center of pressure location. In order for the glider to remain stable during flight the center of pressure should not experience any sudden shifting. If the center of pressure does not remain relatively stable then the glider could move in and out of ground effect and lose the aerodynamic advantages from being close to the ground.

The CFD results have been placed into a series of tables which show the lift and drag coefficients at various angles of attack and height-to-chord ratios. The CFD results have also been put into two figures which show the trend of the lift and drag coefficients at each angle of attack.

Table 11 shows the various lift and drag coefficients at the various height-to-chord ratios for the Wortmann FX 63-137 airfoil. At this angle of attack the values of C_l do not increase as the distance from the ground decreases. The drag on the airfoil was reduced as the airfoil approached the ground. The drag was expected to be reduced as it approached the ground for an angle of attack of 0 due to the reduction in pressure on the lower surface of the airfoil.

Table 11: Lift and Drag Coefficients of FX 63-137 at AOA 0 degrees

C_d	H/C	C_l
0.009450	**0.05**	0.728
0.008380	**0.15**	0.935
0.008863	**0.3**	0.953
0.009223	**0.4**	0.957
0.009900	**0.6**	0.964
0.010516	**0.8**	0.966
0.011129	**1**	0.967

The second angle of attack tested was 2 degrees and the values of the lift and drag coefficient were put into Table 12. The airfoil is beginning to show the characteristics of ground effect flight in terms of lift and drag. The lift is increased when the airfoil is within 4.5 cm of the ground, then the lift reaches a constant as it approaches the height-to-chord ratio of 1. The drag values show a constant decrease as the airfoil is lowered closer to the ground.

Table 12: Lift and Drag Coefficients of FX 63-137 at AOA 2 degrees

C_d	H/C	C_l
0.008793	**0.05**	1.282
0.009359	**0.15**	1.214
0.010187	**0.3**	1.190
0.010696	**0.4**	1.188
0.011648	**0.6**	1.192
0.012540	**0.8**	1.197
0.013455	**1**	1.200

Table 13 shows the lift and drag coefficients for the angle of attack of 4 degrees. The airfoil continues to show the beginning characteristics of ground effect as there is again an increase in lift within 4 cm of the ground and then the lift coefficient levels off as the height-to-chord ratio approaches 1. The drag forces however are now showing a more dramatic decrease in drag the closer the airfoil is to the ground.

Table 13: Lift and Drag Coefficients of FX 63-137 at AOA 4 degrees

C_d	H/C	C_l
0.011312	**0.05**	1.481
0.011766	**0.15**	1.411
0.012673	**0.3**	1.389
0.013287	**0.4**	1.389
0.014508	**0.6**	1.399
0.015763	**0.8**	1.410
0.017202	**1**	1.428

The lift and drag coefficient at an angle of attack of 6 degrees are shown in Table 14. Again at this angle of attack the lift is also increased as the airfoil is closer to the

ground, which is expected. The drag decreased when the airfoil is closer to the ground which is common with the trend set by the previous angle of attacks.

Table 14: Lift and Drag Coefficients of FX 63-137 at AOA 6 degrees

C_d	H/C	C_l
0.014674	**0.05**	1.618
0.014901	**0.15**	1.576
0.015861	**0.3**	1.569
0.016706	**0.4**	1.580
0.018291	**0.6**	1.602
0.019933	**0.8**	1.621
0.021494	**1**	1.632

Figure 22 gives a visual representation of the coefficient of lift values for the Wortmann FX 63-137 for all of the tested angles of attack. It can be seen that when the angle of attack is greater than zero for the airfoil the lift increases when the airfoil is below the height-to-chord ratio of 0.4. The reason that the lift is so low for the angle of attack of zero is similar to the situation which was present with the experimental results of the NACA airfoil. For this case the airfoil is so low to the ground that the since the airfoil has no angle of attack there is not enough air flowing under the wing to generate as much lift as the wing is capable of. This lift coefficient is significantly higher than that of the NACA 4412 airfoil and this is mostly due to airfoil geometry.

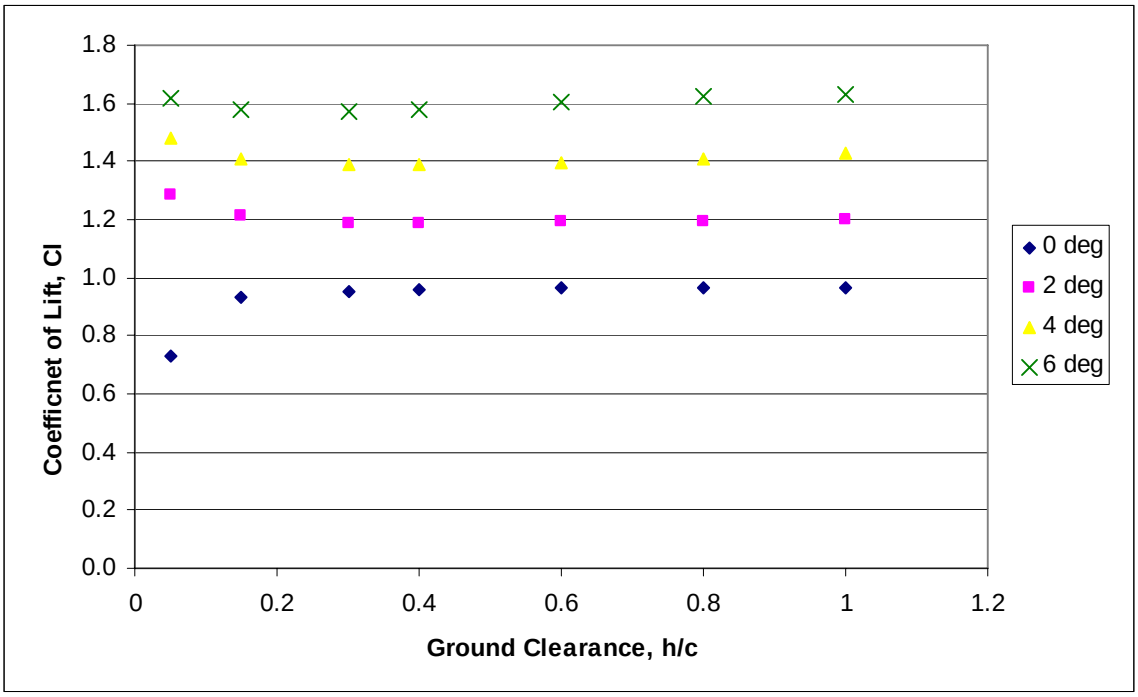

Figure 22: Coefficient of Lift of Wortmann FX 63-137 for Tested Angles of Attack

Figure 23 is a visual representation of the drag coefficient for the Wortmann airfoil at the 4 tested angles of attack. This figure provides a clear visual of the decrease in drag as the airfoil gets closer to the ground. The drag coefficient is more drastic for the greater angle of attack which can be expected since the ground influences the airfoil greater when there is an angle of attack to allow pressure build-up under the airfoil to create the “cushion” of air that is common in ground effect flight.

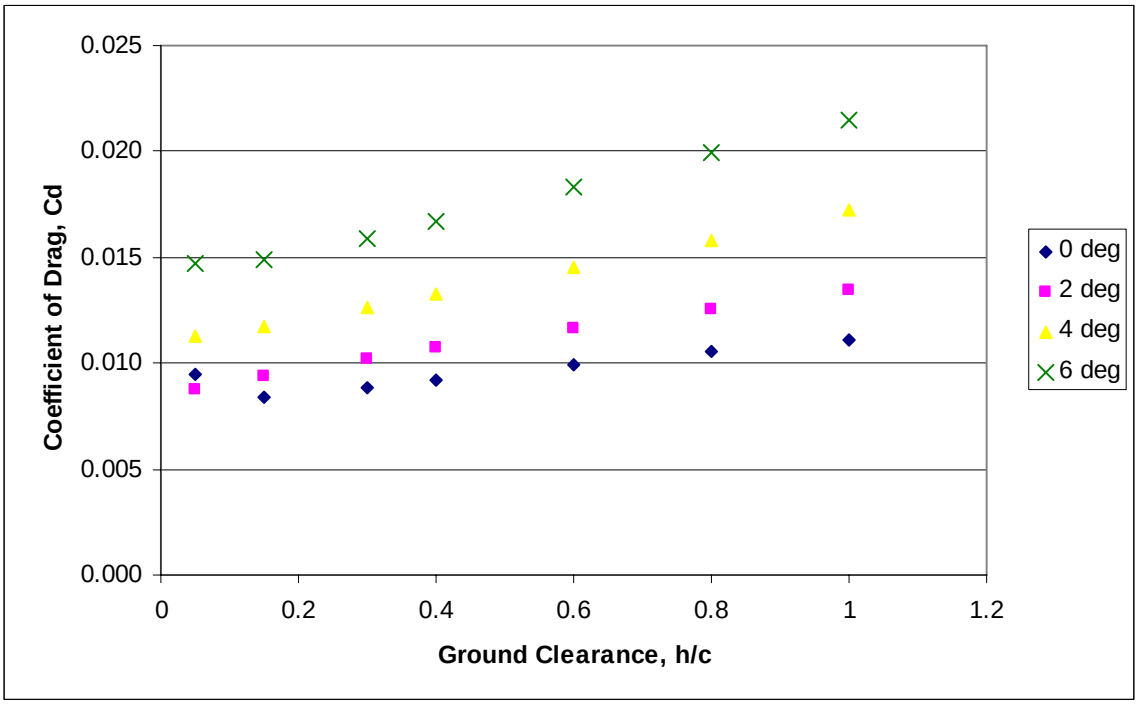

Figure 23: Coefficient of Drag of Wortmann FX 63-137 for Tested Angles of Attack

These drag coefficients are for a two dimensional flow analysis of the selected airfoil. In order to produce the most accurate analysis a three dimensional analysis should be performed on airfoil setups which are of the greatest interest. A three dimensional flow analysis will allow the equations which are being solved by Fluent to be solved in a z-axis as well as the x-axis and y-axis.

Another focus of the research on the Wortmann FX 63-137 is the location of the center of pressure, and how that center of pressure moves with different altitudes and different angles of attack. The behavior of the center of pressure will greatly determine the performance, handling, and other flight characteristics of a recreational glider. Table 15 lists the value for the location of the center of pressure in terms of percentage along the chord length in the x-direction.

The table shows the movement along the x-axis is minimal with change in altitude and is slightly greater in change in angle of attack. The movement of the center of

pressure along the x-axis for just a change in altitude is a maximum at 0 degrees angle of attack and is 7.9 % of the chord length. The minimum change in the center of pressure location is 0.6 % of the chord length at both 2 and 4 degrees.

If the center of pressure locations are averaged over every altitude, then the distance the location will travel when angle of attack is changed can be measured. At an angle of attack of 0 degrees the center of pressure location is the furthest back at 49.2 % of the chord length. The center of pressure locations for the angles of attack between 2 and 6 degrees are closer to each other, and they also represent a more realistic angle of attack for flight. The center of pressure only changes 4.5 % of the chord length from a flight at 2 degrees angle of attack and 6 degrees angle of attack.

Table 15: Wortmann FX 63-137 $X_{C.P.}$ Location for Tested Angles of Attack

AOA	0 deg	2 deg	4 deg	6 deg
H/C	X c.p.	X c.p.	X c.p.	X c.p.
0.05	0.557	0.442	0.416	0.400
0.15	0.490	0.438	0.411	0.394
0.3	0.480	0.436	0.410	0.392
0.4	0.479	0.436	0.409	0.391
0.6	0.478	0.437	0.409	0.391
0.8	0.479	0.437	0.410	0.391
1	0.480	0.438	0.411	0.391

Figure 24 gives more of a visual representation of what is happening with the location of the center of pressure. It can be seen in the figure that if a steady level flight of one angle of attack can be maintained, the center of pressure remains relatively constant for different altitudes. The stability of the center of pressure is important when the altitude is changing since the surface that the recreational glider would be flying over could have variations in it.

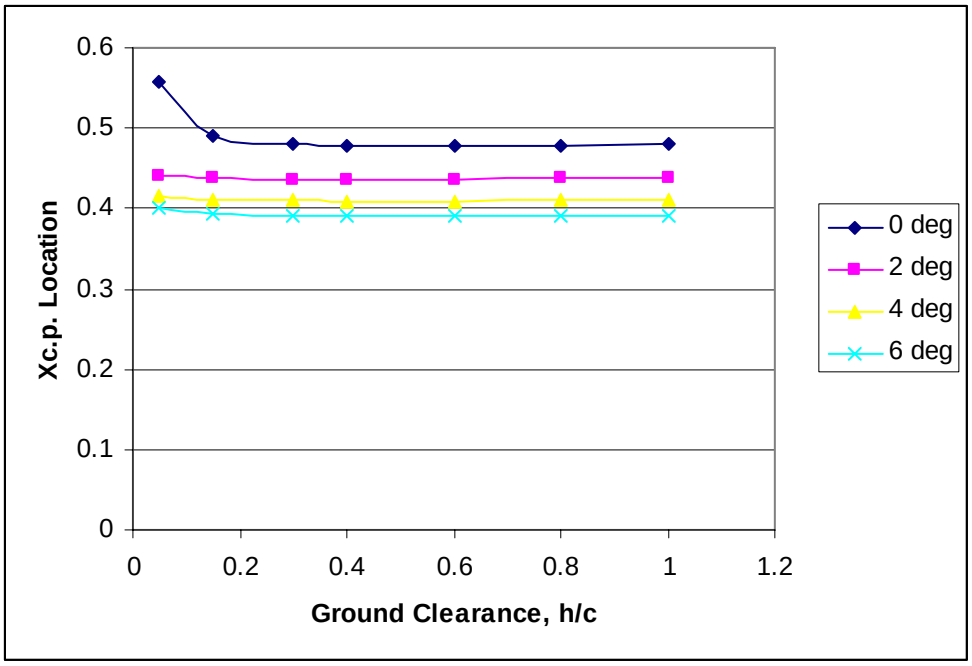

Figure 24: $X_{C.P.}$ Location of Wortmann FX 63-137 for Tested Angles of Attack

There will need to be further research performed on the center of pressure movement throughout flight. This however will not be able to be done until there is a working model which can be tested. The stability of this glider will be the most difficult design aspect if the advantages from ground effect are the governing the flight regime of the aircraft.

Chapter 6.0 Conclusions and Recommendations

The first analysis of the Wortmann FX 63-137 airfoil as the selected airfoil for the proposed recreational glider being designed by CIRA turned up results that were somewhat expected based on previous knowledge of ground effect flight. Ground effect flight characteristics could be seen when looking at the coefficient of lift and drag results. The Wortmann FX 63-137 showed an increase in lift as the airfoil approached the ground, especially at the angles of attack of 4 and 6 degrees. The drag forces experienced by the airfoil were also lowered as the airfoil was lowered toward the ground.

The center of pressure location was also an area of concern as was discussed earlier. The shifting of the center of pressure was found to be minimal but only while at a steady angle of attack. When the angle of attack changed, so did the location of the center of pressure. This is an area of concern which must be addressed further when experimental testing begins.

The experiment which was chosen to verify the techniques used in CFD did not show the lift and drag behavior which was expected but instead showed an increase in drag as the airfoil approached the ground. The lift force on the NACA 4412 showed very little or no change at all when exposed to ground effect. This experiment recreation in CFD was also a two dimensional analysis of a three dimensional experiment, which will introduce errors into the coefficient.

The three dimensional case which was run showed that the percent difference in drag was significantly reduced as compared to a two dimensional analysis. The trend developed with the two dimensional model should be used in order to select airfoil setups which should be further analyzed using three dimensional flow.

This experiment did fill a valid need of data which could be recreated to a degree for a specific airfoil in order to verify computational research being done on a different airfoil. This computational research can now be used as a starting point in order to decide if it the airfoil and test setup should be recreated experimentally.

6.1 Recommendations

Now that computational results have been obtained for the first selected airfoil, the Wortmann FX 63-137, further decisions need to be made on how the design process with move forward. The first step is to experimentally verify these computational results, similarly to the way the experiment using the NACA 4412 airfoil was compared using CFD. In order to design such an experiment, an apparatus needs to be built which can be used to test the airfoil in a similar way that was done in the NACA 4412 experiment. The experiment should show the same general trend of the lift increasing as the airfoil approached the ground, as well as a decrease in drag at the same time.

If the experimental data verifies the computational data, then the first design process can progress forward. The initial recreational glider design could be used if the computational results are proven accurate. This design would provide a baseline of what areas of the craft needed to be addressed in order to achieve successful flight. Areas that should be of concern are sudden shifting of the center of pressure, as well as if the airfoil produces enough lift in order to obtain and maintain flight.

Research should be performed on several individual aspects of the recreational glider. One topic that should be covered is the effect of slots in order to bleed off lift from so that the airfoil does not suddenly experience increases in lift, which could cause an unsteady flight path. Also there may be a way to permanently alter the airfoil in order to

help maintain a more stable center of pressure, such as a trailing edge modification. Flight control is also an area of interest, as it has been with previous ground effect aircraft since the aircraft is being operated so close to the ground. The flight controls and handling capabilities of such a recreational glider could prove to be very complicated. These are just several areas of research that should be looked at as the initial testing for this recreational glider is beginning.

Chapter 7.0 References

[1]. Rozhdestvensky, K.V., *Aerodynamics of a Lifting System in Extreme Ground Effect*. Springer, Berlin, 2000, pp. 1.

[2]. Wieselsberger, C. "Wing Resistance Near the Ground." 1921, Technical Memorandum – 77.

[3]. Raymond, A.E. "Ground Influence on Aerofoils." 1921, NACA Technical Note – 67.

[4]. Reid, E.G. "A Full-Scale Investigation of Ground Effect." 1927, NACA Technical Report – 265.

[5]. Calkins, D.E. "Feasibility Study of a Hybrid Airship Operating in Ground Effect." *Journal of Aircraft*, Vol. 14, No. 8, August 1977, pp. 809-815.

[6]. Ollila, R.G. "Historical Review of WIG Vehicles." *Journal of Hydronautics*, Vol. 14, No. 3, July 1980, pp. 65-76.

[7]. Lange, R.H., and J.W. Moore. "Large Wing-in-Ground Effect Transport Aircraft." *Journal of Aircraft*, Vol. 17, No. 4, April 1980, pp. 260-266.

[8]. Cole, W. "The Pelican: A Big Bird for the Long Haul." *Boeing Frontiers Online*. Vol. 1, Issue 5, September 2002. accessed 4 June 2007 <http://www.boeing.com/news/frontiers/archive/2002/september/i_pw.html>.

[9]. Ailor, W.H., and W.R. Eberle. "Configuration Effects on the Lift of a Body in Close Ground Proximity." *Journal of Aircraft*, Vol 13, No. 8, August 1976, pp. 584-589.

[10]. Chawla, M.D., Edwards, L.C., and M.E. Franke. "Wind-Tunnel Investigation of Wing-in-Ground Effects." *Journal of Aircraft*, Vol. 27, No. 4, April 1990, pp. 289-293.

[11]. Ahmed, N.A., and J. Goonarantne. "Lift Augmentation of a Low-Aspect-Ratio Thick Wing in Ground." *Journal of Aircraft*, Vol. 39, No. 2, March-April 2002, pp. 381-384.

[12]. Zerihan, J., and X. Zhang. "Aerodynamics of a Single Element Wing in Ground Effect." *Journal of Aircraft*, Vol. 37, No. 6, November-December 2000, pp. 1058-1064.

[13]. Zhang, X., and J. Zerihan. "Off-Surface Aerodynamic Measurements of a Wing in Ground Effect." *Journal of Aircraft*, Vol. 40, No. 4, July-August 2003, pp. 716-725.

[14]. Ahmed, M.R., Kohama, Y., and T. Takasaki. "Aerodynamics of a NACA4412 Airfoil in Ground Effect." *AIAA Journal*, Vol. 45, No. 1, Jan. 2007, pp. 37-47.

[15]. Saunders, G.H. "Aerodynamic Characteristics of Wings in Ground Proximity." *Canadian Aeronautics and Space Journal*, June 1965, pp. 185-192.

[16]. Tuck, E.O. "A Nonlinear Unsteady One-Dimensional Theory for Wings in Extreme Ground Effect." *Journal of Fluid Mechanics*, Vol. 98, Part 1, 1980, pp. 33-47.

[17]. Tan, C.H. and A. Plotkin. "Lifting-Line Solution for a Symmetrical Thin Wing in Ground Effect." *AIAA Journal*, Vol. 24, No. 7, July 1986, pp. 1193-1194.

[18]. Chen, Y.S, and W.G. Schweikhard. “Dynamic Ground Effects on a Two-Dimensional Flat Plate.” *Journal of Aircraft*, Vol. 22, No. 7, July 1985, pp. 638-640.
[19]. Nuhait, A.O., and D.T. Mook. “Numerical Simulation of Wings in Steady and Unsteady Ground Effects.” *Journal of Aircraft*, Vol. 26, No. 12, December 1989, pp. 1081-1089.
[20]. Nuhait, A.O., and M.F. Zedan. “Numerical Simulation of Unsteady Flow Induced by a Flat Plate Moving Near Ground.” *Journal of Aircraft*, Vol. 30, No. 5, Sept.-Oct. 1993, pp. 611-617.
[21]. Coulliette, C. and A. Plotkin. “Aerofoil ground effect revisited.” *Aeronautical Journal*, February 1996, pp. 65-74.
[22]. Fonseca, G.F., Bodstein, G.C.R., and M.H. Hirata. “Numerical Simulation of Inviscid Incompressible Two-Dimensional Airfoil – Vortex Interaction in Ground Effect.” *Journal of Aircraft*, Vol. 40, No. 4, July-August 2003, pp. 653-661.
[23]. Staufenbiel, R.W., and U.J. Schlichting. “Stability of Airplanes in Ground Effect.” *Journal of Aircraft*, Vol. 25, No. 4, April 1988, pp. 289-294.
[24]. De Divitiis, N. “Performance and Stability of a Winged Vehicle in Ground Effect.” *Journal of Aircraft*, Vol. 42, No. 1, January-February 2005, pp. 148-157.
[25]. Hsiun, C.H., and C. K. Chen. “Aerodynamic Characteristics of a Two-Dimensional Airfoil with Ground Effect.” *Journal of Aircraft*, Vol. 33, No. 2, March-April 1996, pp. 386-392.
[26]. Steinbach, D. “Comment on Aerodynamic Characteristics of a Two-Dimensional Airfoil with Ground Effect.” *Journal of Aircraft*, Vol. 34, No. 3, May-June 1997, pp. 455-456.
[27]. Barber, T.J., Leonardi, E., and R.D. Archer. “A Technical Note on the Appropriate CFD Boundary Conditions for the Prediction of Ground Effect aerodynamics.” *The Aeronautical Journal*, November 1999, pp. 545-547.
[28]. Barber, T.J., Leonardi, E., and R.D. Archer. “Causes for Discrepancies in Ground Effect Analyses.” *The Aeronautical Journal*, December 2002, pp. 653-667.
[29]. Barber, T. “Aerodynamic Ground Effect: A Case Study of the Integration of CFD and Experiments.” *International Journal of Vehicle Design*, Vol. 40, No. 4, 2006, pp. 299-316.
[30]. Chun, H.H., and R.H. Chang. “Turbulence Flow Simulation for Wings in Ground Effect with Two Ground Conditions: Fixed and Moving Ground.” *International Journal of Maritime Engineering*, 2003, pp. 211-228.
[31]. Young, D.F., Munson, B.R. and Okiishi, T.H. *A Brief Introduction to Fluid Mechanics*. Wiley, New York, 1997, pp. 447.
[32]. Abbott, I. H., and A.E. Von Doenhoff, *Theory of Wing Sections*. 1st edition, Dover, New York, 1959, pp. 488-489.

Appendix

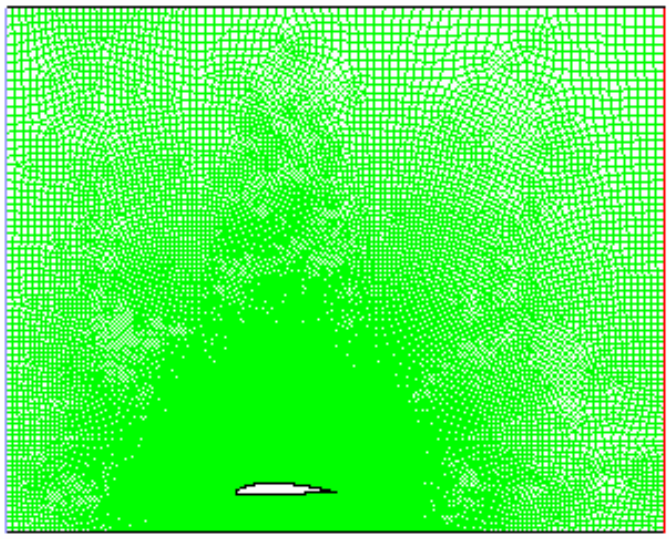

Figure A 1: Grid Setup for NACA 4412 at AOA 0 deg H/C 0.4

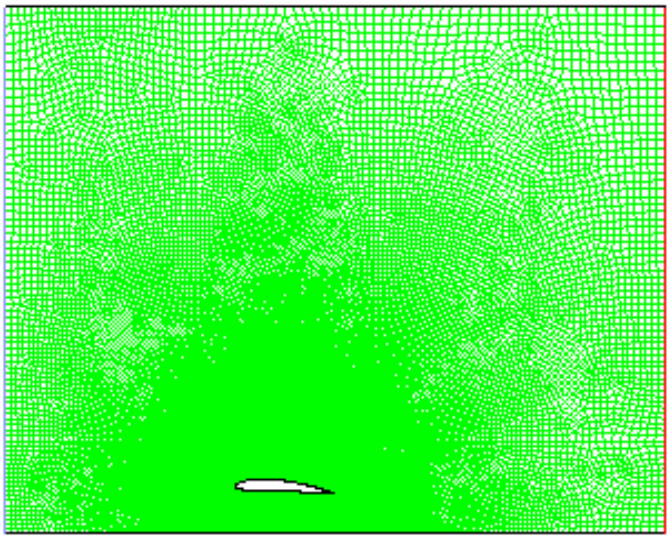

Figure A 2: Grid Setup for NACA 4412 at AOA 4 deg H/C 0.4

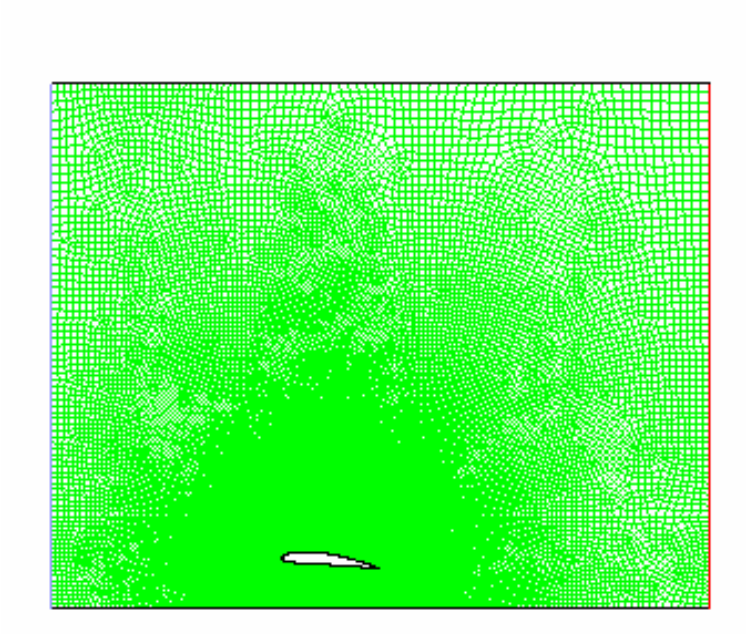

Figure A 3: Grid Setup for NACA 4412 at AOA 6 deg H/C 0.4

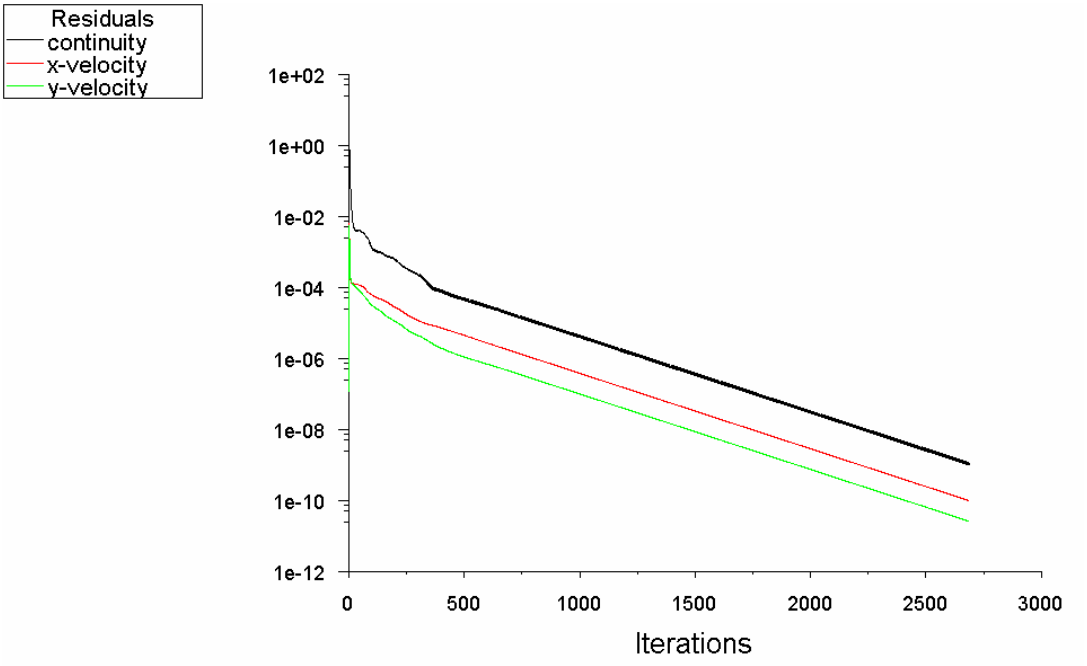

Figure A 4: Example of Convergence of Residuals for NACA 4412 at AOA 2 deg H/C 0.4

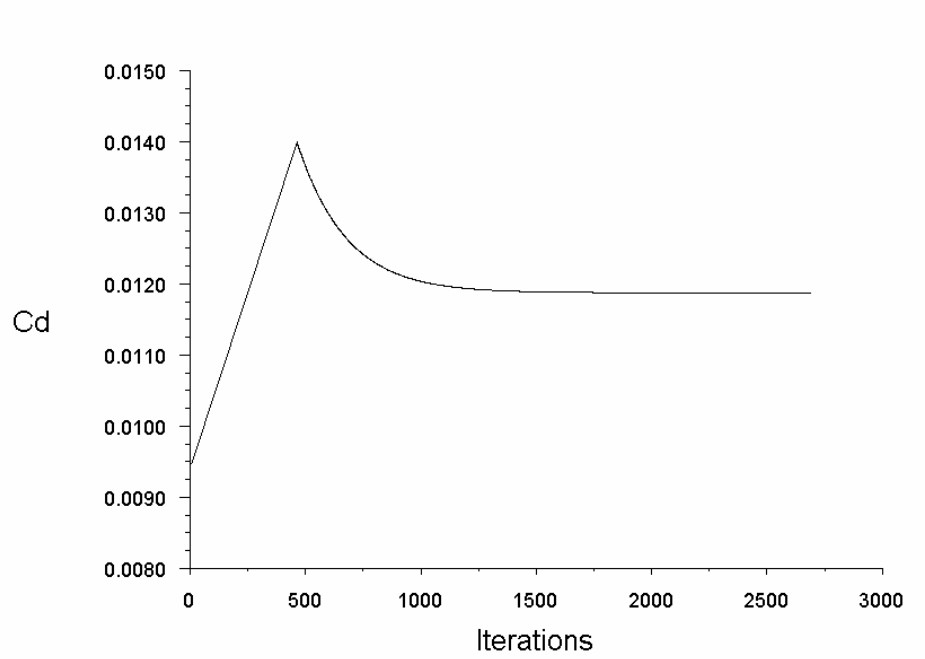

Figure A 5: Example of Convergence of C_d for NACA 4412 at AOA 2 deg H/C 0.4

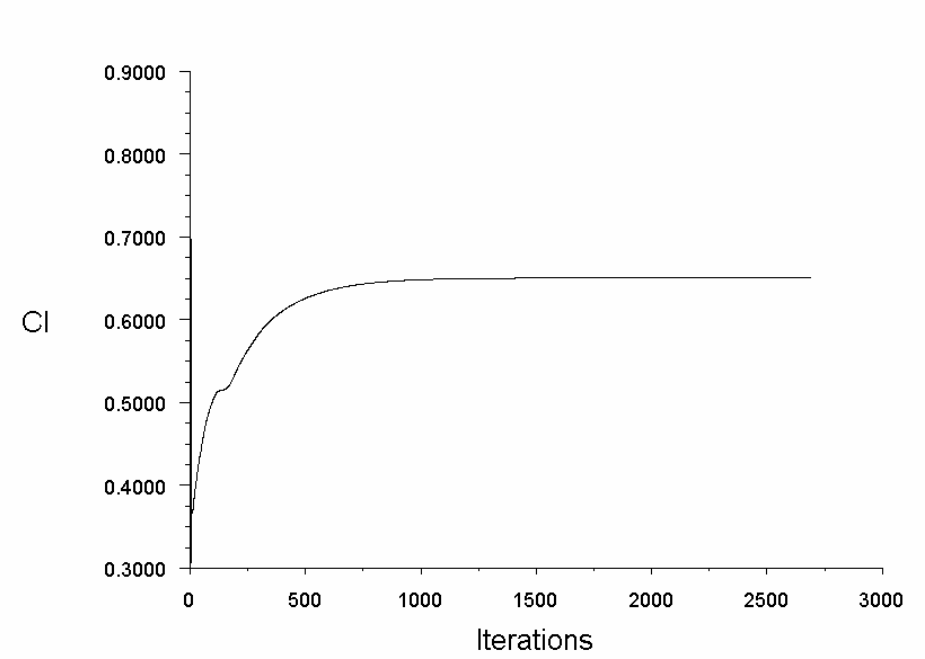

Figure A 6: Example of Convergence of C_l for NACA 4412 at AOA 2 deg H/C 0.4

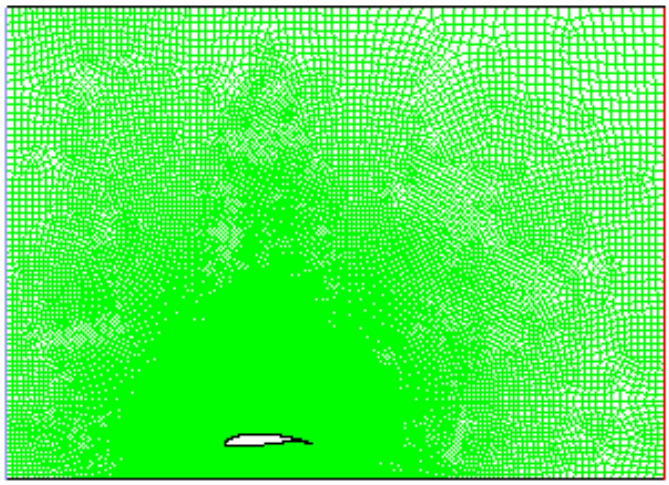

Figure A 7: Grid Setup for Wortmann FX 63-137 at AOA 0 deg H/C 0.4

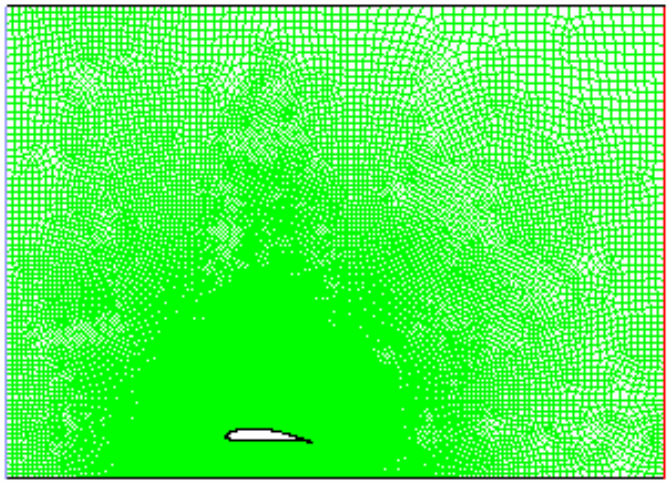

Figure A 8: Grid Setup for Wortmann FX 63-137 at AOA 4 deg H/C 0.4

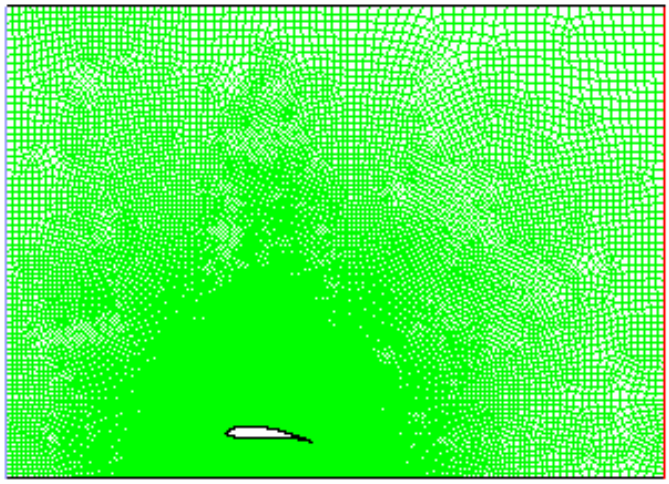

Figure A 9: Grid Setup for Wortmann FX 63-137 at AOA 6 deg H/C 0.4

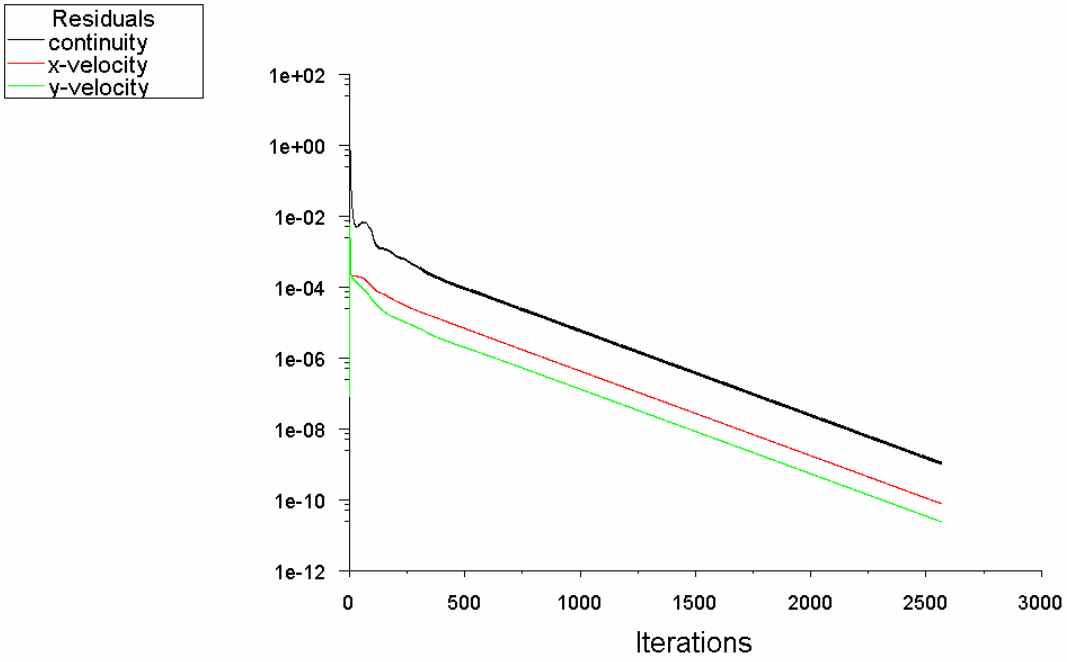

Figure A 10: Example of Convergence of Residuals for Wortmann FX 63-137 at AOA 2 deg H/C 0.4

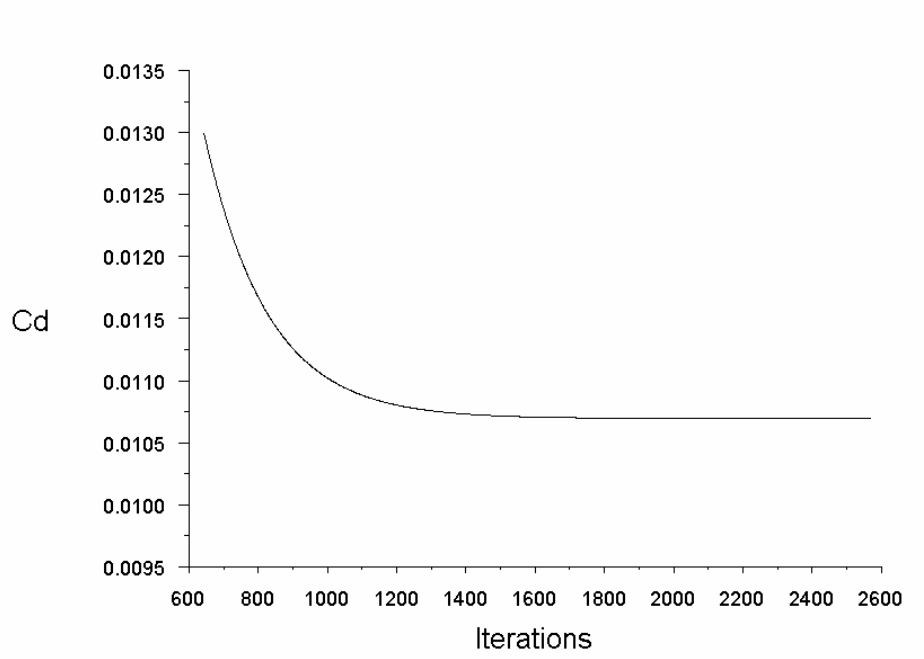

Figure A 11: Example of Convergence of C_d for Wortmann FX 63-137 at AOA 2 deg H/C 0.4

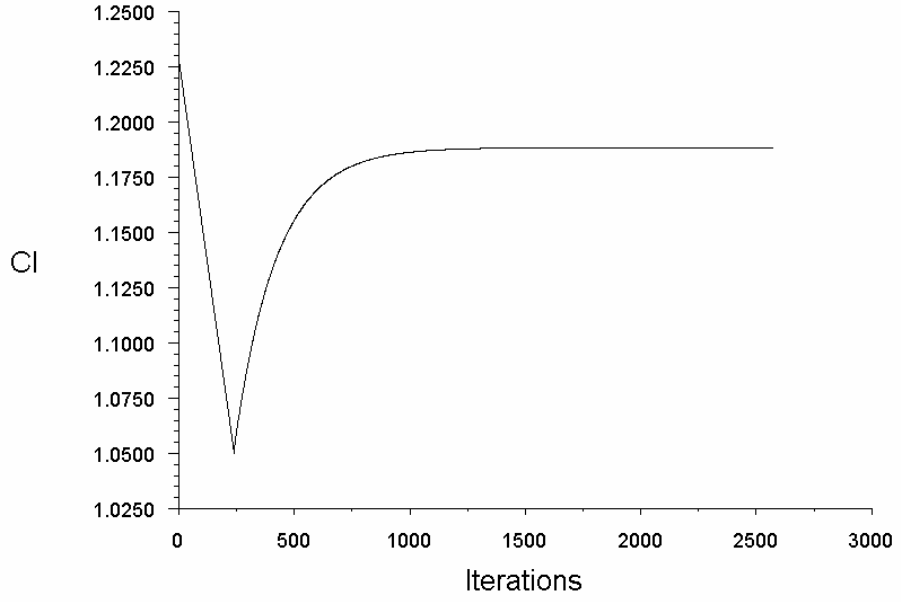

Figure A 12: Example of Convergence of C_l for Wortmann FX 63-137 at AOA 2 deg H/C 0.4